Serum concentration and expression of Reg IV in patients with esophageal cancer: Age-related elevation of serum Reg IV concentration

NAOHIDE OUE[1], TSUYOSHI NOGUCHI[2], KATSUHIRO ANAMI[1], KAZUHIRO SENTANI[1], NAOYA SAKAMOTO[1], NAOHIRO URAOKA[1], YUTA WAKAMATSU[1], HIROKI SASAKI[3] and WATARU YASUI[1]

[1]Department of Molecular Pathology, Hiroshima University Graduate School of Biomedical Sciences, Hiroshima;
[2]Department of Gastrointestinal Surgery, Oita University Faculty of Medicine, Oita;
[3]Genetics Division, National Cancer Center Research Institute, Tokyo, Japan

Received September 29, 2010; Accepted December 29, 2010

DOI: 10.3892/ol.2011.239

Abstract. *Regenerating islet-derived family, member 4* (*REG4*, which encodes Reg IV) is a marker for cancer and inflammatory bowel disease. This study aimed to investigate the diagnostic utility of Reg IV measurement in sera from esophageal cancer patients. Reg IV expression was examined in 269 esophageal cancer samples by immunostaining and the Reg IV levels in sera were measured from 65 patients with esophageal squamous cell carcinoma (SCC) by enzyme-linked immunosorbent assay. No Reg IV staining was detected in 255 SCC and 4 small cell carcinoma samples, whereas Reg IV was stained in 4 of 10 (40%) adenocarcinoma samples. Serum Reg IV concentration in esophageal SCC patients was significantly higher compared to that of the control subjects (P=0.0003). A significant correlation between serum Reg IV concentration and age was found in control subjects (P<0.0001). When serum Reg IV concentration was analyzed according to age, the distribution of serum Reg IV concentration in patients with esophageal SCC was similar to that of the control subjects. These results suggest that Reg IV expression is highly specific for adenocarcinoma of the esophagus. Further investigation is required to clarify whether Reg IV serves as a serum tumor marker for esophageal cancer.

Introduction

Regenerating islet-derived family, member 4 (*REG4*, which encodes Reg IV) is a member of the *REG* gene family, which constitutes a multi-gene family belonging to the calcium-dependent lectin superfamily. *REG4* was originally identified by high-throughput sequence analysis of a large inflammatory bowel disease cDNA library (1). Previously a serial analysis of gene expression in four primary gastric cancer tissues was performed and a number of gastric cancer-specific genes were identified (2,3). Of these genes, *REG4* is a candidate gene for cancer-specific expression in patients with gastric cancer. Our previous immunohistochemical analysis showed that Reg IV was expressed in 30% of gastric cancers and was associated with intestinal mucin phenotype and neuroendocrine differentiation (4). A number of immunohistochemical analyses of Reg IV have been reported in human cancers, including lung, breast, pancreas, colorectal, prostate, salivary gland, kidney, urinary bladder and gallbladder cancer (4-11). These analyses indicate that Reg IV is expressed in adenocarcinoma cells showing intestinal mucin differentiation. Reg IV staining also aids in the diagnosis of gastrointestinal signet ring cell carcinoma, a unique subtype of adenocarcinoma (12). By contrast, little is known about Reg IV expression in other histological types of cancer, such as squamous cell carcinoma (SCC).

In addition to adenocarcinoma, Reg IV expression has been reported in neuroendocrine neoplasms, including gastrointestinal and renal carcinoids (4,10,13). Reg IV expression is also found in small cell carcinoma of the lung (14). However, Reg IV expression in small cell carcinoma of the esophagus has yet to be investigated.

Reg IV is a secreted protein and a novel biomarker for gastric cancer (15). The diagnostic sensitivity of serum Reg IV was superior to that of serum carcinoembryonic antigen or carbohydrate antigen 19-9. Serum Reg IV serves as a tumor marker for colorectal, pancreatic and prostate cancer (5,7,10). The data support the hypothesis that Reg IV protein is a potentially novel serum tumor marker for a wide range of malignancies. However, the serum concentration of Reg IV in esophageal cancer has yet to be measured.

In the present study, the expression and distribution of Reg IV in human esophageal cancers, including SCC, adenocarcinoma and small cell carcinoma, was examined by immunohistochemistry. Previously two Reg IV staining patterns, i.e., mucin-like and strong perinuclear staining were reported (4). Mucin-like staining is observed in goblet cells

Correspondence to: Dr Wataru Yasui, Department of Molecular Pathology, Hiroshima University Graduate School of Biomedical Sciences, 1-2-3 Kasumi, Minami-ku, Hiroshima 734-8551, Japan
E-mail: wyasui@hiroshima-u.ac.jp

Key words: Reg IV, esophageal cancer, tumor marker, immunohistochemistry

and goblet cell-like vesicles of cancer cells. These cells are positive for MUC2 (a marker of goblet cells). By contrast, strong perinuclear staining is detected in neuroendocrine cells. These cells are positive for chromogranin A (a marker of neuroendocrine cells). Therefore, the coexpression of Reg IV and MUC2 or chromogranin A was examined. Additionally, the Reg IV levels in sera from patients with esophageal cancer were measured using an enzyme-linked immunosorbent assay (ELISA) to investigate the potential diagnostic utility of Reg IV measurement.

Materials and methods

Tissue samples. Primary tumor samples from 279 patients with esophageal cancer (35 females and 244 males; age range 36-84 years, mean 65) and serum samples from 65 patients with esophageal cancer (8 females and 57 males; age range 49-82 years, mean 65) were collected. The patients had undergone curative resection between 1990 and 2002 at Oita University Hospital, Oita, Japan. Only patients without pre-operative radio- or chemotherapy and without clinical evidence of distant metastasis were enrolled in the study. The histologic classification was based on the World Health Organization system. Tumor staging was performed according to the TNM stage grouping system. For strict privacy protection, identifying information for the samples was removed prior to being analyzed in accordance with the Ethical Guidelines for Human Genome/Gene Research enacted by the Japanese Government.

For quantitative reverse transcription-polymerase chain reaction (RT-PCR), 10 primary esophageal cancer tissue samples and their corresponding non-neoplastic mucosa samples were used. The 10 esophageal cancer samples were all SCC. The samples were obtained at the time of resection, immediately frozen in liquid nitrogen and stored at -80˚C until use. It was microscopically confirmed that the tumor specimens consisted mainly (>50%) of carcinoma tissue.

The 269 primary esophageal cancer tissue samples were used for immunohistochemical analysis. The samples were archival formalin-fixed, paraffin-embedded tissues. These 269 esophageal cancer samples were classified histologically as SCC (n=255), adenocarcinoma (n=10) or small cell carcinoma (n=4).

Serum samples were used to measure Reg IV levels using ELISA. All 65 serum samples were obtained from patients with esophageal SCC prior to surgery and before initiation of therapy. Primary esophageal SCC tissue samples from all 65 patients with esophageal cancer were available for immunohistochemical analysis. The control serum samples were obtained from 133 healthy individuals (92 females and 41 males; age range 21-80 years, mean 51). Control subjects were randomly selected from individuals visiting hospitals for regular health checks or due to certain symptoms, such as appetite loss or epigastralgia. The control subjects were confirmed to be free of malignancy by gastrointestinal endoscopy and biopsy. The serum samples were stored at -80˚C until analysis.

Quantitative RT-PCR. Total RNA was extracted with an RNeasy mini kit (Qiagen, Valencia, CA, USA) and 1 μg of total RNA was converted to cDNA with a First Strand cDNA synthesis kit (Amersham Biosciences, Piscataway, NJ, USA). Quantitation of *REG4* mRNA levels was performed by real-time fluorescence detection as previously described (2). In brief, PCR was performed with a SYBR-Green PCR Core Reagents kit (Applied Biosystems, Foster City, CA, USA). Real-time detection of the emission intensity of SYBR-Green bound to double-stranded DNA was performed with an ABI PRISM 7700 Sequence Detection System (Applied Biosystems) as previously described (16). ACTB-specific PCR products were amplified from the same RNA samples and served as an internal control.

Immunohistochemistry. Formalin-fixed, paraffin-embedded samples were sectioned, deparaffinized and stained with hematoxylin and eosin to ensure that the sectioned block contained tumor cells. Adjacent sections were then stained immunohistochemically. The sections were pre-treated by microwaving in citrate buffer for 30 min to retrieve antigenicity. After peroxidase activity was blocked with 3% H_2O_2-methanol for 10 min, the sections were incubated with normal goat serum (Dako, Carpinteria, CA, USA) for 20 min to block non-specific antibody binding. The sections were incubated with a primary antibody against Reg IV (rabbit polyclonal antibody, diluted 1:50; anti-Reg IV antibody was raised and characterized in our laboratory) (4), MUC2 (1:50; Novocastra, Newcastle, UK) or chromogranin A (1:50; Novocastra) for 1 h at room temperature, followed by incubation with peroxidase-labeled anti-rabbit or anti-mouse IgG for 1 h. Staining was completed with a 10-min incubation in a substrate-chromogen solution. The sections were counterstained with 0.1% hematoxylin. The specificity of the Reg IV antibody was previously characterized (4). Staining of each antibody was considered positive if any tumor cells were stained.

Enzyme-linked immunosorbent assay. For the measurement of serum Reg IV concentration, a sandwich ELISA method was developed as previously described (15). First, polystyrene microtiter plates were coated with mouse monoclonal anti-Reg IV antibody (R&D Systems, Abingdon, UK) by overnight incubation of 50 μl/125 ng/well antibody diluted in Tris buffer (pH 7.4). The plates were then washed three times with wash buffer. After the plates were blocked with 1% milk in phosphate-buffered saline, 50 μl of recombinant Reg IV standard or sample was added to each well and incubated overnight at 4˚C. After three washes, 50 μl of biotinylated goat polyclonal anti-Reg IV antibody (R&D Systems) in assay buffer [1% bovine serum albumin (BSA), Tris buffer (pH 7.4) and 0.05% normal goat serum] was added to each well (75 ng antibody/well). The mixture was then incubated for 1 h with agitation at 37˚C and washed three times with wash buffer. The plates were incubated with 50 μl/well alkaline phosphatase-conjugated streptavidin (Dako) diluted 1:2,000 in diluent containing 1% BSA and Tris buffer (pH 7.4) for 1 h at 37˚C and washed three times. Color development was performed with the addition of pNPP chromogenic substrate (Sigma-Aldrich, St. Louis, MO, USA) followed by incubation at 37˚C for 1 h. Absorbance at 405 nm was measured with an ELISA plate reader. As a reference standard, known concentrations of human recombinant Reg IV from 0 to 30 ng/ml were tested in triplicate.

Statistical methods. Differences in the serum Reg IV concentration between two groups were tested using the non-

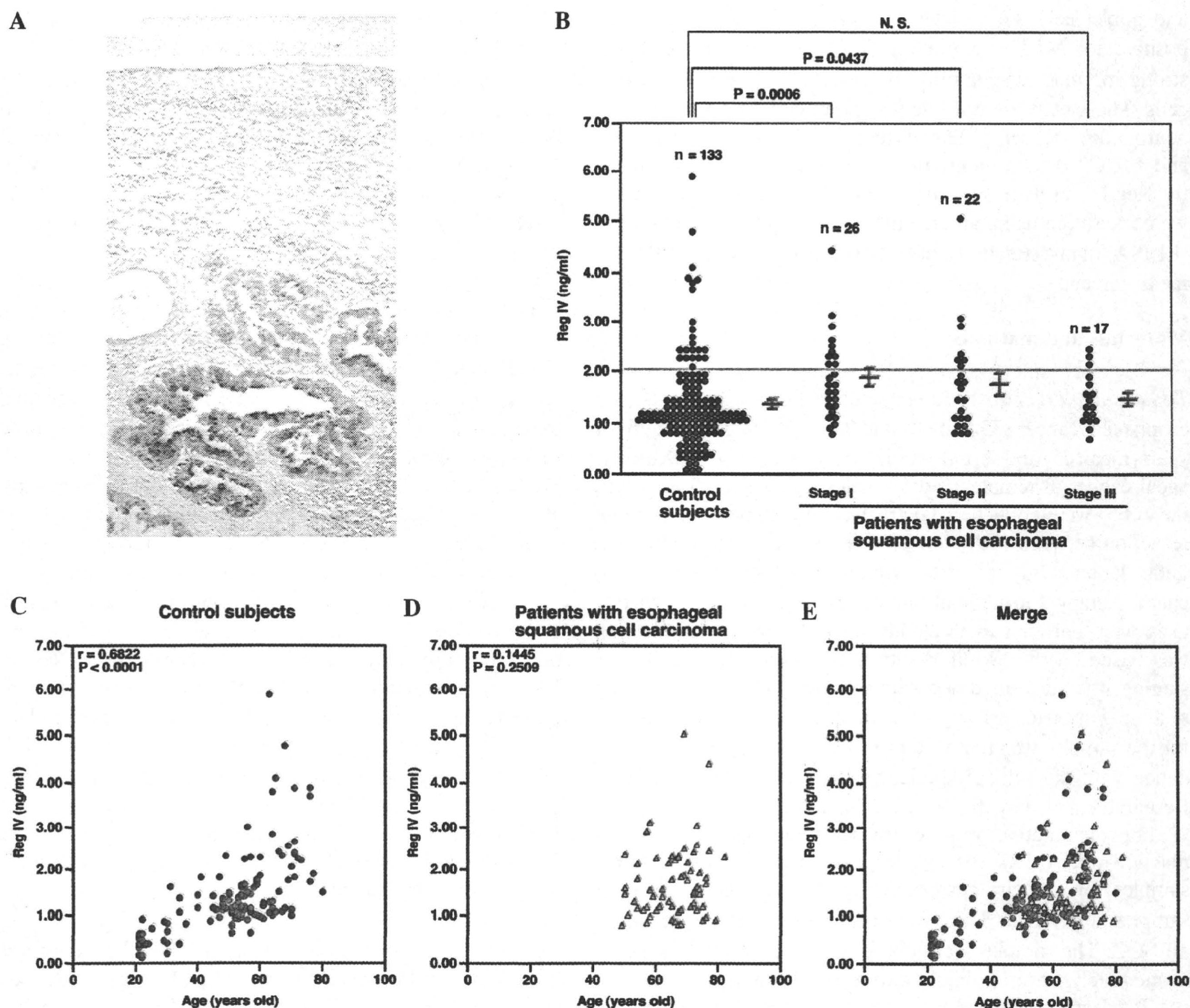

Figure 1. Immunostaining and serum concentration of Reg IV in esophageal cancer. (A) Immunostaining of Reg IV in esophageal adenocarcinoma (original magnification, x100). Reg IV staining is observed in goblet cell-like vesicles of adenocarcinoma cells. (B) Enzyme-linked immunosorbent assay of serum samples from 133 control subjects and 65 patients with esophageal squamous cell carcinoma (SCC). The yellow bar indicates the cut-off levels defined on the basis of a previous study (2 ng/ml) (15). The red bars indicate the mean ± SE. Differences in the serum concentration of Reg IV between two groups were tested using the Mann-Whitney U test. (C) Correlation between the serum concentrations of Reg IV and age in control subjects. The correlation was examined using Spearman's rank correlation test. (D) Correlation between the serum concentrations of Reg IV and age in patients with esophageal SCC. The correlation was examined using Spearman's rank correlation. (E) Panel (C) was merged with panel (D).

parametric Mann-Whitney U test. Correlations between the serum Reg IV concentration and age or gender were assessed using Spearman's rank correlation test. $P<0.05$ was considered to be statistically significant.

Results

Expression of Reg IV in esophageal cancer. An immunohistochemical analysis of Reg IV was performed in 269 human esophageal cancer tissue samples. Although esophageal SCC is the most frequent subtype of esophageal cancer in Asian countries, no Reg IV staining was detected in any of the 255 esophageal SCC samples. Quantitative RT-PCR of *REG4* was performed in 10 esophageal SCC samples; however, no *REG4* expression was found. By contrast, Reg IV was stained in 4 of 10 (40%) adenocarcinoma samples (Fig. 1A). The Reg IV staining was mucin-like; no perinuclear staining was noted. It was confirmed that tumor cells showing mucin-like staining of Reg IV were positive for MUC2 and negative for chromogranin A (data not shown). Although extensive chromogranin A staining was observed in the 4 samples of small cell carcinoma, no Reg IV staining was found (data not shown). Reg IV staining was also not found in corresponding non-neoplastic squamous cells (Fig. 1A).

Serum Reg IV concentration in patients with esophageal squamous cell carcinoma and control subjects. Serum Reg IV levels in 133 control subjects and 65 patients with esophageal SCC measured by ELISA are shown in Fig. 1B. The serum Reg IV concentration of control subjects measured in the

present study (mean ± SE, 1.38±0.08 ng/ml) was higher than that measured in our previous study (0.52±0.05 ng/ml) (15). The correlation between the serum concentration of Reg IV and age or gender was investigated. Although the serum concentration of Reg IV did not correlate with age in our previous study (15), serum concentration was higher in elderly compared to that in young control subjects. Spearman's rank correlation test showed a significant correlation between serum Reg IV and age (r=0.4362, P<0.0001) (Fig. 1C). In our previous study, the cut-off level for Reg IV was set at 2 ng/ml (15). A high level of Reg IV concentration was found in 13 of 23 (57%) control subjects who were more than 65 years old.

Serum Reg IV concentration in esophageal SCC patients at stage I (n=26, 1.88±0.16 ng/ml, P=0.0006, Mann-Whitney U test) and stage II (n=22, 1.76±0.21 ng/ml, P=0.0437, Mann-Whitney U test) was significantly higher than that of the control subjects (Fig. 1B). By contrast, the serum Reg IV concentration in esophageal SCC patients at stage III was not significantly elevated (n=17, 1.48±0.11 ng/ml, P=0.1329, Mann-Whitney U test). In total, serum Reg IV concentration in esophageal SCC patients (n=65, 1.74±0.10 ng/ml) was significantly higher compared to that of the control subjects (P=0.0003, Mann-Whitney U test).

In the present study, no Reg IV expression was detected in esophageal SCC by quantitative RT-PCR and immunohistochemistry. However, serum Reg IV concentration in esophageal SCC patients was significantly higher compared to that of the control subjects. Discrepancy between immunostaining and ELISA results is not likely due only to methodological differences. Spearman's rank correlation test showed that there was no significant correlation between serum Reg IV concentration in esophageal SCC patients and age (r=0.1445, P=0.2509) (Fig. 1D). Additionally, when the distribution of serum Reg IV concentration in esophageal SCC patients was compared to that of the control subjects, it was not significantly different (Fig. 1E).

Discussion

This study aimed to investigate the expression of Reg IV in esophageal cancer. Although Reg IV staining was not detected in esophageal SCC and small cell carcinoma samples, it was present in 40% of adenocarcinoma samples. We confirmed that the adenocarcinoma cells were also positive for MUC2. In our previous study, Reg IV expression was not found in renal cell carcinoma and was noted in only 1% of urothelial carcinoma, neither of which are adenocarcinomas (10). Taken together, these results indicate that the expression of Reg IV is highly specific for adenocarcinoma.

Although Reg IV expression was not found in esophageal SCC at the mRNA and protein levels, serum Reg IV concentrations in esophageal SCC patients at stages I and II were significantly higher compared to those of the control subjects. Spearman's rank correlation test showed a significant correlation between serum Reg IV and age in control subjects. In the ELISA analysis, the mean age of the control subjects (51 years) was younger than that of patients with esophageal SCC (65 years), suggesting that the elevation of the serum concentration of Reg IV in esophageal SCC is age-related and not due to esophageal SCC. Notably, the distribution of serum Reg IV concentration in esophageal SCC patients did not show a significant difference from that noted in the control subjects.

We are unable to thoroughly explain this age-related elevation of serum Reg IV concentration. A number of lines of evidence have suggested that Reg IV protein detected in serum samples is derived from cancer cells. In pancreatic adenocarcinoma patients, postoperative serum Reg IV levels were reduced to within normal range 3 or 4 weeks following tumor resection (5). The Reg IV concentration in serum samples from patients with gastric cancer showing Reg IV-positive immunostaining was significantly higher compared to that with gastric cancer showing Reg IV-negative immunostaining (15). Although the control subjects were confirmed to be free of malignancy by gastrointestinal endoscopy and biopsy, the possibility that the control subjects had cancer cannot be excluded. To address these issues, serum samples from cancer-free subjects confirmed by autopsy should be analyzed.

Another possible explanation for the age-related elevation of serum Reg IV concentration is Reg IV expression in intestinal metaplasia of the stomach. In our previous study, normal stomach cells were not stained by Reg IV, however, extensive staining of Reg IV was observed in intestinal metaplasia of the stomach (4). Since the incidence and prevalence of intestinal metaplasia of the stomach increase with age, age-related elevation of serum Reg IV concentration may be due to Reg IV expression in intestinal metaplasia of the stomach.

In conclusion, we showed that the expression of Reg IV is highly specific for adenocarcinoma, but is not specific for SCC or small cell carcinoma. Although serum Reg IV concentration in esophageal SCC patients was significantly higher than that in control subjects, we hypothesize that serum Reg IV is not suitable as a tumor marker for esophageal SCC detection. The reason for the apparent age-related elevation of serum Reg IV concentration in esophageal SCC patients has yet to be elucidated and further investigation is required to clarify the potential utility of serum Reg IV measurement.

Acknowledgements

We thank Mr. Shinichi Norimura for the excellent technical assistance and advice. This study was carried out with the kind cooperation of the Research Center for Molecular Medicine, Faculty of Medicine, Hiroshima University. We thank the Analysis Center of Life Science, Hiroshima University, for the use of their facilities. This study was supported in part by Grants-in-Aid for Cancer Research from the Ministry of Education, Culture, Science, Sports and Technology of Japan, and from the Ministry of Health, Labor and Welfare of Japan.

References

1. Hartupee JC, Zhang H, Bonaldo MF, Soares MB and Dieckgraefe BK: Isolation and characterization of a cDNA encoding a novel member of the human regenerating protein family: Reg IV. Biochim Biophys Acta 1518: 287-293, 2001.
2. Oue N, Hamai Y, Mitani Y, Matsumura S, Oshimo Y, Aung PP, Kuraoka K, Nakayama H and Yasui W: Gene expression profile of gastric carcinoma: identification of genes and tags potentially involved in invasion, metastasis, and carcinogenesis by serial analysis of gene expression. Cancer Res 64: 2397-2405, 2004.

3. Aung PP, Oue N, Mitani Y, Nakayama H, Yoshida K, Noguchi T, Bosserhoff AK and Yasui W: Systematic search for gastric cancer-specific genes based on SAGE data: melanoma inhibitory activity and matrix metalloproteinase-10 are novel prognostic factors in patients with gastric cancer. Oncogene 25: 2546-2557, 2006.
4. Oue N, Mitani Y, Aung PP, Sakakura C, Takeshima Y, Kaneko M, Noguchi T, Nakayama H and Yasui W: Expression and localization of Reg IV in human neoplastic and non-neoplastic tissues: Reg IV expression is associated with intestinal and neuroendocrine differentiation in gastric adenocarcinoma. J Pathol 207: 185-198, 2005.
5. Takehara A, Eguchi H, Ohigashi H, Ishikawa O, Kasugai T, Hosokawa M, Katagiri T, Nakamura Y and Nakagawa H: Novel tumor marker REG4 detected in serum of patients with resectable pancreatic cancer and feasibility for antibody therapy targeting REG4. Cancer Sci 97: 1191-1197, 2006.
6. Nakata K, Nagai E, Ohuchida K, Aishima S, Hayashi A, Miyasaka Y, Yu J, Mizumoto K, Tanaka M and Tsuneyoshi M: REG4 is associated with carcinogenesis in the 'intestinal' pathway of intraductal papillary mucinous neoplasms. Mod Pathol 22: 460-468, 2009.
7. Oue N, Kuniyasu H, Noguchi T, Sentani K, Ito M, Tanaka S, Setoyama T, Sakakura C, Natsugoe S and Yasui W: Serum concentration of Reg IV in patients with colorectal cancer: overexpression and high serum levels of Reg IV are associated with liver metastasis. Oncology 72: 371-380, 2007.
8. Ohara S, Oue N, Matsubara A, Mita K, Hasegawa Y, Hayashi T, Usui T, Amatya VJ, Takeshima Y, Kuniyasu H and Yasui W: Reg IV is an independent prognostic factor for relapse in patients with clinically localized prostate cancer. Cancer Sci 99: 1570-1577, 2008.
9. Sasahira T, Oue N, Kirita T, Luo Y, Bhawal UK, Fujii K, Yasui W and Kuniyasu H: Reg IV expression is associated with cell growth and prognosis of adenoid cystic carcinoma in the salivary gland. Histopathology 53: 667-675, 2008.
10. Hayashi T, Matsubara A, Ohara S, Mita K, Hasegawa Y, Usui T, Arihiro K, Norimura S, Sentani K, Oue N and Yasui W: Immunohistochemical analysis of Reg IV in urogenital organs: Frequent expression of Reg IV in prostate cancer and potential utility as serum tumor marker. Oncol Rep 21: 95-100, 2009.
11. Tamura H, Ohtsuka M, Washiro M, Kimura F, Shimizu H, Yoshidome H, Kato A, Seki N and Miyazaki M: Reg IV expression and clinicopathologic features of gallbladder carcinoma. Hum Pathol 40: 1686-1692, 2009.
12. Sentani K, Oue N, Tashiro T, Sakamoto N, Nishisaka T, Fukuhara T, Taniyama K, Matsuura H, Arihiro K, Ochiai A and Yasui W: Immunohistochemical staining of Reg IV and claudin-18 is useful in the diagnosis of gastrointestinal signet ring cell carcinoma. Am J Surg Pathol 32: 1182-1189, 2008.
13. Sentani K, Oue N, Noguchi T, Sakamoto N, Matsusaki K and Yasui W: Immunostaining of gastric cancer with neuroendocrine differentiation: Reg IV-positive neuroendocrine cells are associated with gastrin, serotonin, pancreatic polypeptide and somatostatin. Pathol Int 60: 291-297, 2010.
14. Heiskala K, Arola J, Heiskala M and Andersson LC: Expression of Reg IV and Hath1 in neuroendocrine neoplasms. Histol Histopathol 25: 63-72, 2010.
15. Mitani Y, Oue N, Matsumura S, Yoshida K, Noguchi T, Ito M, Tanaka S, Kuniyasu H, Kamata N and Yasui W: Reg IV is a serum biomarker for gastric cancer patients and predicts response to 5-fluorouracil-based chemotherapy. Oncogene 26: 4383-4393, 2007.
16. Kondo T, Oue N, Yoshida K, Mitani Y, Naka K, Nakayama H and Yasui W: Expression of POT1 is associated with tumor stage and telomere length in gastric carcinoma. Cancer Res 64: 523-529, 2004.

uicc
global cancer control

IJC
International Journal of Cancer

Anti-stromal therapy with imatinib inhibits growth and metastasis of gastric carcinoma in an orthotopic nude mouse model

Tomonori Sumida[1], Yasuhiko Kitadai[1], Kei Shinagawa[1], Miwako Tanaka[1], Michiyo Kodama[1], Mayu Ohnishi[1], Eiji Ohara[1], Shinji Tanaka[2], Wataru Yasui[3] and Kazuaki Chayama[1]

[1] Department of Medicine and Molecular Science, Graduate School of Biomedical Sciences, Hiroshima University, Hiroshima, Japan
[2] Department of Endoscopy, Hiroshima University Hospital, Hiroshima, Japan
[3] Department of Molecular Pathology, Graduate School of Biomedical Sciences, Hiroshima University, Hiroshima, Japan

Recent studies have revealed that platelet-derived growth factor (PDGF) plays a role in promoting progressive tumor growth in several organs; however, whether PDGF plays such a role in gastric carcinoma is undetermined. We examined whether inhibition of PDGF receptor (PDGF-R) tyrosine kinase signaling by imatinib affects tumor growth and metastasis in an orthotopic nude mouse model of human gastric carcinoma. TMK-1 human gastric carcinoma cells were injected into the gastric wall of nude mice. Groups of mice ($n = 10$ each) received sterile water (control), low-dose imatinib (50 mg/kg/day), high-dose imatinib (200 mg/kg/day), cancer chemotherapeutic agent irinotecan (5 mg/kg/week), or imatinib (50 mg/kg/day or 200 mg/kg/day) and irinotecan (5 mg/kg/week) in combination for 28 days. Tumor growth and metastasis were assessed. Resected tumors were analyzed immunohistochemically. Carcinoma-associated fibroblasts, pericytes and lymphatic endothelial cells in stroma expressed high levels of PDGF-R; carcinoma cells did not. Treatment with imatinib alone did not inhibit tumor growth and metastasis; however, treatment with irinotecan alone or combined with imatinib significantly inhibited tumor growth. Only treatment with high-dose imatinib and irinotecan in combination inhibited lymph node and peritoneal metastases. Immunohistochemically, only imatinib alone or in combination with irinotecan was shown to significantly decrease the stromal reaction, microvessel area and pericyte coverage of tumor microvessels. These effects were marked with high-dose imatinib. In conclusion, administration of PDGF-R tyrosine kinase inhibitor in combination with irinotecan appears to impair the progressive growth of gastric carcinoma by blockade of PDGF-R signaling pathways in stromal cells.

Recent studies in tumor biology have shown that tumor growth and metastasis are determined not only by cancer cells, but also by a variety of stromal cells. The stroma constitutes a large part of most solid tumors, and the cancer-stromal cell interaction contributes functionally to tumor growth and metastasis.[1,2] Tumor stroma contains many different cell types, including activated fibroblasts (myofibroblasts), endothelial cells and inflammatory cells. It has become clear that activated fibroblasts in cancer stroma are prominent modifiers of tumor progression. As such, they are called carcinoma-associated fibroblasts (CAFs).[3] Although the mechanisms that regulate activation of fibroblasts and their accumulation in tumors are not fully understood, platelet-derived growth factor (PDGF), transforming growth factor-β and fibroblast growth factor (FGF)-2 are known to be partly involved in this process.[4]

PDGF and PDGF receptor (PDGF-R) are expressed in many types of human neoplasm, including neoplasm of the prostate,[5] lung,[6] colon[7] and breast.[8,9] PDGF is a dimeric protein of the following molecular variants: PDGF-AA, PDGF-BB, PDGF-AB, PDGF-CC and PDGF-DD.[10] The α-receptor binds all possible forms of PDGF except PDGF-DD, whereas PDGF-Rβ preferentially binds PDGF-BB. PDGF-R signaling is reported to increase proliferation of tumor cells in an autocrine manner[11] and to stimulate angiogenesis,[12] recruit pericytes[11,13] and control interstitial fluid pressure (IFP) in stroma, influencing transvascular transport of chemotherapeutic agents in a paracrine manner.[14] Receptor tyrosine kinases have been proposed as potential targets for antitumor therapy. Imatinib mesylate (also known as STI571 or Gleevec) is a protein-tyrosine kinase inhibitor of the 2-phenylaminopyrimidine class that was developed initially for its

Key words: gastric carcinoma, platelet-derived growth factor receptor, carcinoma-associated fibroblast
Grant sponsors: Ministry of Education, Culture, Science, Sports and Technology of Japan (Grants-in-Aid for Cancer Research), Ministry of Health, Labor and Welfare of Japan
DOI: 10.1002/ijc.25812
History: Received 7 May 2010; Accepted 11 Nov 2010; Online 2 Dec 2010
Correspondence to: Yasuhiko Kitadai, Department of Medicine and Molecular Science, Graduate School of Biomedical Sciences, Hiroshima University, 1-2-3 Kasumi, Minami-ku, Hiroshima 734-8551, Japan, Tel: +81-82-257-5193, Fax: +81-82-257-5194, E-mail: kitadai@hiroshima-u.ac.jp

selectivity against Bcr-Abl fusion protein present in nearly all patients with chronic myeloid leukemia.[15] Additional tyrosine kinases are inhibited by imatinib: c-kit, the receptor for kit ligand (KL) and two structurally similar PDGF-Rs (PDGF-Rα and PDGF-Rβ) and DDRs (DDR1 and DDR2).[16,17] Imatinib therapy is well tolerated and leads to remission in patients with c-kit-positive gastrointestinal stromal tumor containing gain-of-function mutations in c-kit.[18] Imatinib is also reported to inhibit the growth of glioblastoma, dermatofibrosarcoma protuberans, neuroblastoma, Ewing's sarcoma and small cell lung cancer, all of which may exhibit PDGF/PDGF-R or KL/c-kit autocrine growth loops.[19–23] It was reported recently that blockade of paracrine PDGF-R signaling pathways in tumor-associated endothelial cells could serve as a novel therapy for many neoplasms.[24,25] In addition to endothelial cells that form the tumor vasculature, attention is now focused on other elements of the stromal compartment, *i.e.*, CAFs and vascular pericytes.[26]

In this study, we examined the therapeutic effect of imatinib administered as a single agent or in combination with chemotherapeutic agent irinotecan against human gastric carcinoma cells growing in an orthotopic nude mice model, paying particular attention to tumor stroma. Irinotecan has been evaluated alone and in combined therapy in multiple trials, with promising results and good tolerance in patients with advanced gastric carcinoma.[27]

Material and Methods

Human gastric carcinoma cell lines and culture conditions

The TMK-1 cell line (poorly differentiated adenocarcinoma) was kindly provided by Dr. E. Tahara (Hiroshima University, Hiroshima, Japan). The KKLS cell line (undifferentiated carcinoma) was kindly provided by Dr. Y. Takahashi (Chiba University, Chiba, Japan). Human osteosarcoma cell line MG63 (positive control for PDGF-R expression) was obtained from the Health Science Research Resources Bank, Osaka, Japan. These cell lines were maintained in RPMI 1640 (Nissui Co., Tokyo, Japan) with 10% fetal bovine serum (FBS; Sigma, St. Louis, MO).

Semiquantitative reverse transcription polymerase chain reaction

Total RNA was extracted from gastric carcinoma cell lines with an RNeasy Kit (Qiagen, Tokyo, Japan) according to the manufacturer's instructions. Reverse transcription polymerase chain reaction (RT-PCR) was performed with the isolated RNA (1 μg). cDNA was generated from 1 μg of total RNA with a first-strand cDNA synthesis kit (Amersham Biosciences, Buckinghamshire, UK). Semi-quantitative RT-PCR was performed with an AmpliTag Gold Kit (Roche, Mannheim, Germany) according to the manufacturer's instructions. RT-PCR reactions without reverse transcription showed no specific bands. Respective primer sequences, annealing temperatures and PCR cycles were as follows: PDGF-B forward, CGAGTTGGACCTGAACATGA and PDGF-B reverse, GTCACCGTGGCCTTCTTAAA (PDGF-B PCR product, 339 bp; 58°C; 30 cycles); PDGF-Rβ forward, AGCTACCCCT CAAGGAATCATAG and PDGF-Rβ reverse, CTCTG GTGGATGGATTAAGACTG (PDGF-Rβ PCR product, 376 bp; 58°C; 30 cycles); and GAPDH forward, ATCATCC CTGCCTCTACTGG and GAPDH reverse, CCCTCCG ACGCCTGCTTCAC (GAPDH PCR product, 188 bp; 58°C; 28 cycles).

Reagents

Imatinib (imatinib mesylate or Gleevec; Novartis Pharma, Basel, Switzerland) was diluted in sterile water for oral administration. Irinotecan (Camptosar; Pharmacia, North Peapack, NJ) was kept at room temperature and dissolved in 0.9% NaCl on the day of intraperitoneal injection. Primary antibodies were purchased as follows: polyclonal rabbit anti-PDGF-Rβ, polyclonal rabbit anti-phosphorylated PDGF-Rβ (p-PDGF-Rβ), polyclonal rabbit anti-PDGF-BB subunit from Santa Cruz Biotechnology (Santa Cruz, CA); rat anti-mouse CD31 from BD PharMingen (San Diego, CA); mouse anti-desmin monoclonal antibody from Molecular Probes (Eugene, OR); α-smooth muscle actin (α-SMA) and Ki-67 equivalent antibody (MIB-1) from Dako Cytomation (Carpinteria, CA); monoclonal rat anti-mouse Lyve-1 antibody from R&D Systems (Minneapolis, MN) and polyclonal rabbit anti-mouse type-1 collagen from Novotec (Saint Martin La Garenne, France). The following fluorescent secondary antibodies were used: Alexa 488-conjugated goat anti-rabbit IgG, Alexa 488-conjugated goat anti-rat IgG and Alexa 546-conjugated goat anti-rabbit IgG (all from Molecular Probes).

Western blot analysis

Gastric carcinoma cell lines and MG63 cells were cultured in serum-free culture medium for 1 hr and then stimulated with 10 ng/mL PDGF-BB for 10 min. After three washes with cold phosphate-buffered saline (PBS) containing 1 mmol/L sodium orthovanadate, cells were lysed. Proteins (total protein 20 μg) were separated by SDS-PAGE and transferred to nitrocellulose transfer membranes (Whatman GmbH, Dassel, Germany). The immune complexes were visualized by enhanced chemiluminescence with an ECL Plus Kit (GE Healthcare, Buckinghamshire, UK).

Cell proliferation assay

In vitro growth was measured with a Cell Proliferation Biotrak ELISA System, version 2 (Amersham Biosciences, Piscataway, NJ), according to the manufacturer's instructions. Cells were seeded in a 96-well plate at a density of 1×10^4 cells/well and incubated overnight in 200 μL culture medium containing 10% FBS. After incubation for 24 hr, cells were cultured in serum-free culture medium containing 10 μM BrdU with or without imatinib for 24 hr, and cell proliferation was measured in a plate reader (Microplate Manager 5.2.1, BIO-RAD, Hercules, CA) at 450 nm.

Animals and orthotopic implantation of tumor cells

Male athymic nude BALB/c mice were obtained from Charles River Japan (Tokyo, Japan). The mice were maintained under specific pathogen-free conditions and used at 5 weeks of age. The study was carried out after permission was granted by the Committee on Animal Experimentation of Hiroshima University. KKLS and TMK-1 cells were harvested from subconfluent cultures by brief exposure to 0.25% trypsin and 0.02% ethylenediamine tetraacetic acid. Trypsinization was stopped with medium containing 10% FBS, and the cells were washed once in serum-free medium and resuspended in Hanks' balanced salt solution (HBSS). Only suspensions consisting of single cells with >90% viability were used. To produce gastric tumors, 1×10^6 cells in 50 μL of HBSS were injected into the gastric wall in nude mice under observation with a zoom stereomicroscope.

Treatment of established human gastric carcinoma tumors growing in the gastric wall in nude mice

To evaluate the therapeutic effects of imatinib on stromal cells, we performed preliminary dose-response experiments (optimal biological dose as determined previously).[28–30] Fourteen days after the orthotopic implantation of tumor cells, mice were randomized into three groups: those given water daily (control group), those given 50 mg/kg/day imatinib by oral gavage and those given 200 mg/kg/day imatinib by oral gavage. Treatments continued for 28 days, and the mice were killed on day 29. Excised tumors were used for immunohistochemical analysis.

To evaluate the effect of combination therapy, in a second experiment, mice were randomized to receive 1 of the following 6 treatments ($n = 10$ in each group): (*i*) daily administration of water by oral gavage and weekly intraperitoneal injection of PBS (control group), (*ii*) daily oral gavage of low-dose imatinib (50 mg/kg) and weekly intraperitoneal injection of PBS, (*iii*) daily oral gavage of high-dose imatinib (200 mg/kg) and weekly intraperitoneal injection of PBS, (*iv*) daily oral gavage of water and weekly intraperitoneal injection of irinotecan (5 mg/kg), (*v*) daily oral gavage of low-dose imatinib (50 mg/kg) and weekly intraperitoneal injection of irinotecan (5 mg/kg), (*vi*) daily oral gavage of high-dose imatinib (200 mg/kg) and weekly intraperitoneal injection of irinotecan (5 mg/kg). The mice were treated for 28 days, then killed and subjected to necropsy.

Necropsy procedures and histologic studies

Mice bearing orthotopic tumors were euthanized by methophane. Body weights were recorded. After necropsy, tumors were excised and weighed. For immunohistochemical and hematoxylin and eosin (H&E) staining, one part of the tumor tissue was fixed in formalin and embedded in paraffin, and the other part was embedded in OCT compound (Miles, Elkhart, IN), rapidly frozen in liquid nitrogen and stored at −80°C. All macroscopically enlarged regional (celiac and para-aortal) lymph nodes were harvested, and the presence of metastatic disease was confirmed by histologic examination.

Double immunofluorescence staining for PDGF-Rβ and α-SMA (CAFs), CD31 (vascular endothelial cells), Lyve-1 (lymphatic endothelial cells) or desmin (pericytes)

Fresh-frozen specimens of TMK-1 human gastric carcinoma tissue obtained from nude mice were cut into 8-μm sections and mounted on positively charged slides. In preparation for assays, sections were fixed in ice-cold acetone for 10 min, then washed thrice with PBS for 3 min each. Slides were placed in a humidified chamber and incubated with protein blocking solution (5% normal horse serum and 1% normal goat serum in PBS) for 20 min at room temperature. The slides were incubated overnight at 4°C with primary antibody against α-SMA, CD31, Lyve-1 or desmin. Slides were then rinsed thrice with PBS and incubated for 10 min in protein blocking solution. For desmin staining, slides were incubated overnight at 4°C with Fab fragment goat anti-mouse IgG (Jackson ImmunoResearch Laboratories, West Grove, PA) to block endogenous immunoglobulins. This was followed by a short incubation with protein blocking solution and then by incubation with primary antibody. Slides were incubated for 1 hr at room temperature with Alexa 488-conjugated secondary antibody. Slides were then incubated overnight at 4°C with antibody against PDGF-Rβ or p-PDGF-Rβ. The sections were rinsed thrice with PBS and incubated for 10 min in protein blocking solution. Slides were incubated for 1 hr at room temperature with Alexa 546-conjugated goat anti-rabbit IgG secondary antibody. The samples were then rinsed thrice in PBS and nuclear counterstained with DAPI for 10 min. Samples were again rinsed thrice with PBS, and mounting medium was placed on each sample, which was protected with a glass coverslip. CAFs, endothelial cells or pericytes were identified by green fluorescence, whereas PDGF-Rβ or p-PDGF-Rβ was identified by red fluorescence.

Double immunofluorescence staining for CD31 (vascular endothelial cells) and desmin (pericytes)

To identify endothelial cells, slides were incubated overnight at 4°C with antibody against CD31. This was followed by incubation with Alexa 488-conjugated goat anti-rat IgG secondary antibody, and the slides were again blocked in a blocking solution as described above and incubated with antibody against desmin. After further washing and further blocking with blocking solution, the slides were incubated with Alexa 546-conjugated goat anti-rabbit IgG secondary antibody. Endothelial cells were identified by green fluorescence, whereas pericytes were identified by red fluorescence.

The coverage of pericytes on endothelial cells was determined by counting CD31-positive cells in direct contact with desmin-positive cells in five randomly selected microscopic fields (at 100× magnification).[31]

Immunohistochemical staining and terminal deoxynucleotide transferase-mediated dUTP-biotin nick end labeling (TUNEL)

Immunohistochemistry for α-SMA, Type-1 collagen, Ki-67 or Lyve-1 was performed on formalin-fixed, paraffin-embedded tissues cut into serial 4-μm sections. After deparaffinization and rehydration, tissue sections for staining of α-SMA, Type-1 collagen, Ki-67 or Lyve-1 were pretreated by microwaving them twice for 5 min in Dako REAL Target Retrieval Solution (Dako). Immunohistochemical staining for CD31 was done on fresh-frozen specimens cut into 8-μm sections. Frozen tissue sections were fixed in cold acetone for 10 min. Primary antibodies were applied to the slides and incubated overnight in humidified boxes at 4°C. After incubation for 1 hr at room temperature with corresponding peroxidase-conjugated secondary antibodies, a positive reaction was detected by exposure to stable 3,3′-diaminobenzidine for 5–10 min. Slides were counterstained with hematoxylin for visualization of the nucleus. Apoptotic cells in tissue sections were detected by TUNEL assay with the ApopTag Plus Peroxidase *In Situ* Apoptosis Detection Kit (CHEMICON, Temecula, CA) according to the manufacturer's instructions.

Quantification of the CAF (α-SMA-positive), collagen (Type-1 collagen-positive), microvessel (CD31-positive) and lymphatic vessel (Lyve-1-positive) areas

To evaluate angiogenic and lymphangiogenic activity of the tumors, the respective areas of vascular and lymphatic microvessels were quantified. Ten random fields at 100× magnification were captured for each tumor, and the outline of each vascular or lymphatic microvessel including a lumen was manually traced. The areas were then calculated with the use of NIH ImageJ software (Wayne Rasband, Bethesda, Maryland). The areas of CAF and extracellular matrix (ECM) were also determined from the respective areas of α-SMA-positive or Type-1 collagen-positive staining from 10 optical fields (100× magnification) of different sections.

Determination of the Ki-67 labeling index (Ki-67 LI) and the apoptotic index

The Ki-67 LI was determined by light microscopy at the site of the greatest number of Ki-67-positive cells. Cells were counted in 10 fields at 40× magnification, and the number of positive cells among ~ 1,000 tumor cells was counted and expressed as a percentage. The number of cells undergoing apoptosis was counted in five random 0.81-mm^2 fields at 100× magnification. The apoptotic index was taken as the ratio of positively stained tumor cells and bodies to all tumor cells and expressed as a percentage for each case.

Confocal microscopy

Confocal fluorescence images were collected by using a 20× or 40× objective lens on a Zeiss LSM laser scanning microscopy system (Carl Zeiss, Thornwood, NY) equipped with a motorized Axioplan microscope, argon laser (458/477/488/514 nm, 30 mW), HeNe laser (543 nm, 1 mW), HeNe laser (633 nm, 5 mW), LSM 510 control and image acquisition software and appropriate filters (Chroma Technology Corp., Brattleboro, VT). Confocal images were exported into Adobe Photoshop, and montages were prepared for publication photos.

Statistical analysis

Results are expressed as mean ± SE. Between-group differences in murine body weight, tumor weight and the areas of α-SMA-positive, Type-1 collagen-positive, CD31-positive and Lyve-1-positive cells were analyzed by Wilcoxon/Kruskal-Wallis test. Differences in the incidence of lymph node metastasis, liver metastasis and peritoneal metastasis were analyzed by Fischer's exact test. Differences in the percentages of Ki-67-positive cells and TUNEL-positive cells were analyzed by unpaired Student's *t*-test or χ^2 test as appropriate. A p value of <0.05 was considered statistically significant.

Results

Expression of PDGF-B and PDGF-Rβ in human gastric carcinoma cell lines

RT-PCR and Western blotting revealed that, under culture conditions, gastric carcinoma cells expressed PDGF-B mRNA, the level of which was higher in TMK-1 cells than in KKLS cells (Fig. 1*a*). PDGF-Rβ was expressed by MG63 cells but not by TMK-1 and KKLS cell lines (Figs. 1*a* and 1*b*). Phosphorylation of PDGF-Rβ in MG63 cells was inhibited by 1 μM imatinib (Fig. 1*c*).

Effect of imatinib on the growth of gastric carcinoma cell lines

To assess the effect of imatinib on growth of gastric carcinoma cell lines *in vitro*, cell proliferation assay was conducted. The reported clinically effective plasma concentration of imatinib is 1–5 μM.[32] Cell proliferation assay revealed no inhibition of gastric carcinoma cell growth after treatment with imatinib even when the concentration of imatinib was increased to 10 μM (Fig. 1*d*).

Expression of PDGF-B and PDGF-Rβ in human gastric carcinoma cells growing in the gastric wall of nude mice

In our orthotopic nude mouse models of KKLS and TMK-1 tumors, tumor cells were shown by immunofluorescence to express PDGF-B but not PDGF-Rβ. The expression level of PDGF-B protein was higher in TMK-1 cells than in KKLS cells (Figs. 2*a* and 2*e*). PDGF-Rβ immunoreactivity was predominant in the tumor stroma (Figs. 2*b* and 2*f*). Because the stroma of TMK-1 tumors expressed p-PDGF-Rβ (Fig. 2*g*), and it was more abundant than that of KKLS tumors (Figs. 2*d* and 2*h*), we used the TMK-1 cell line to identify which cell type in tumor stroma expresses PDGF-Rβ. We did this by double immunofluorescence staining for PDGF-Rβ and α-SMA (CAFs), CD31 (vascular endothelial cells),

Cancer Cell Biology

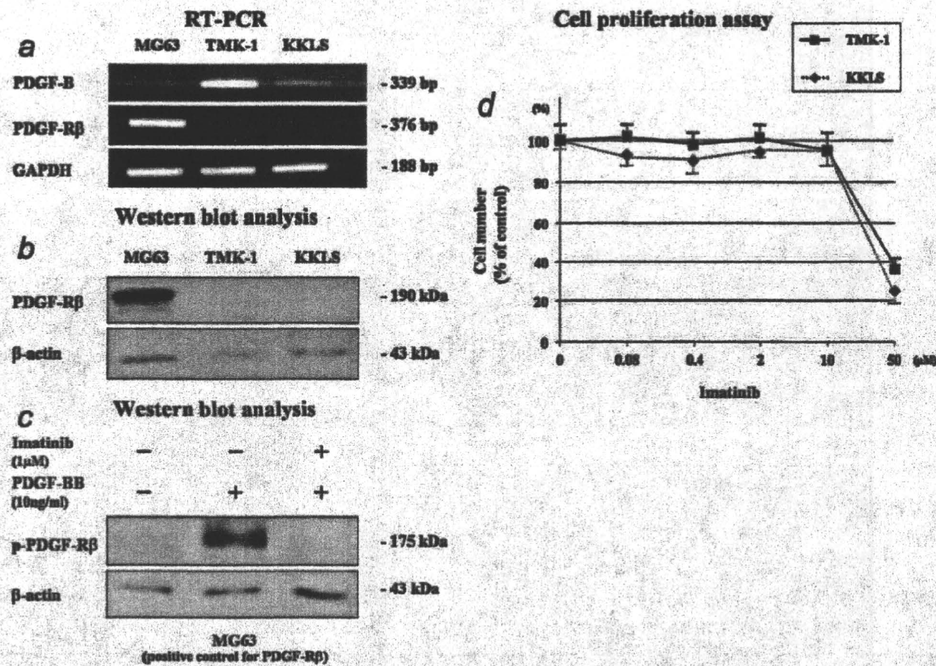

Figure 1. Reverse transcription polymerase chain reaction (RT-PCR) (*a*) and Western blot analysis (*b* and *c*) for expression of PDGF-B and PDGF-Rβ in gastric carcinoma cell lines. In MG63 cell line (positive control for PDGF-R expression), phosphorylation of PDGF-Rβ was inhibited by 1 μM imatinib (*c*). A dose-response curve for imatinib and the effect of growth inhibition *in vitro* in gastric carcinoma cell lines (*d*).

desmin (pericytes) or Lyve-1 (lymphatic endothelial cells). PDGF-Rβ protein co-localized with α-SMA protein, indicating CAFs expressed PDGF-Rβ (Fig. 2*i*). CD31-positive endothelial cells were covered by PDGF-Rβ-positive cells (Fig. 2*j*), which expressed desmin (Fig. 2*k*), indicating that pericytes expressed PDGF-Rβ. Lymphatic endothelial cells stained positively for Lyve-1. Lyve-1 protein also co-localized with PDGF-Rβ protein, suggesting that lymphatic endothelial cells expressed PDGF-Rβ (Fig. 2*l*).

Effect of imatinib on tumor stroma

When we examined the dose effect of imatinib on the inhibition of PDGF-Rβ phosphorylation in stromal cells, we found that the level of PDGF-Rβ expressed by CAFs in orthotopic TMK-1 tumors did not change with treatment (Fig. 3*a*). In contrast, phosphorylation of PDGF-Rβ was markedly inhibited in tumors of mice treated with high-dose imatinib (Fig. 3*b*). The stromal reaction in tumors was evaluated as the area of α-SMA-positive or Type-1 collagen-positive lesions. The effects of imatinib treatment on pericyte coverage of tumor-associated endothelial cells were evaluated by double immunofluorescence staining with anti-CD31 antibody and anti-desmin antibody. We noted morphologic differences between pericytes in the control group and pericytes in the imatinib treatment groups. Pericytes in the control group were enlarged and overlapped each other, whereas pericytes treated with imatinib were very thin (Fig. 3*c*). The stromal reaction was significantly reduced in mice treated with imatinib in comparison to that in control group mice (Figs. 4*a* and 4*b*). These effects were more remarkable in the high-dose imatinib treatment group than in the low-dose imatinib treatment group (Fig. 4*a*).

We also evaluated the dose effect of imatinib on tumor-associated microvessels. The vascular microvessel area (CD31-positive area) was significantly reduced in mice treated with imatinib in comparison with that in control group mice. This effect did not differ significantly between the low-dose and high-dose imatinib treatment groups (Fig. 4*c*). A decrease in the lymphatic vessel area (Lyve-1-positive area) was observed only in the group of mice treated with high-dose imatinib (Fig. 4*d*).

Treatment of human gastric carcinoma growing in the gastric wall of nude mice

We next determined the effects of imatinib, irinotecan and imatinib and irinotecan in combination on the growth and metastasis of TMK-1 human gastric carcinoma cells implanted in the gastric wall of nude mice. The tumor incidence was 100% in all treatment groups. Toxicity of the various treatment regimens was assessed on the basis of change in body weight. Oral administration of imatinib, intraperitoneal injection of irinotecan and administration of the two drugs in

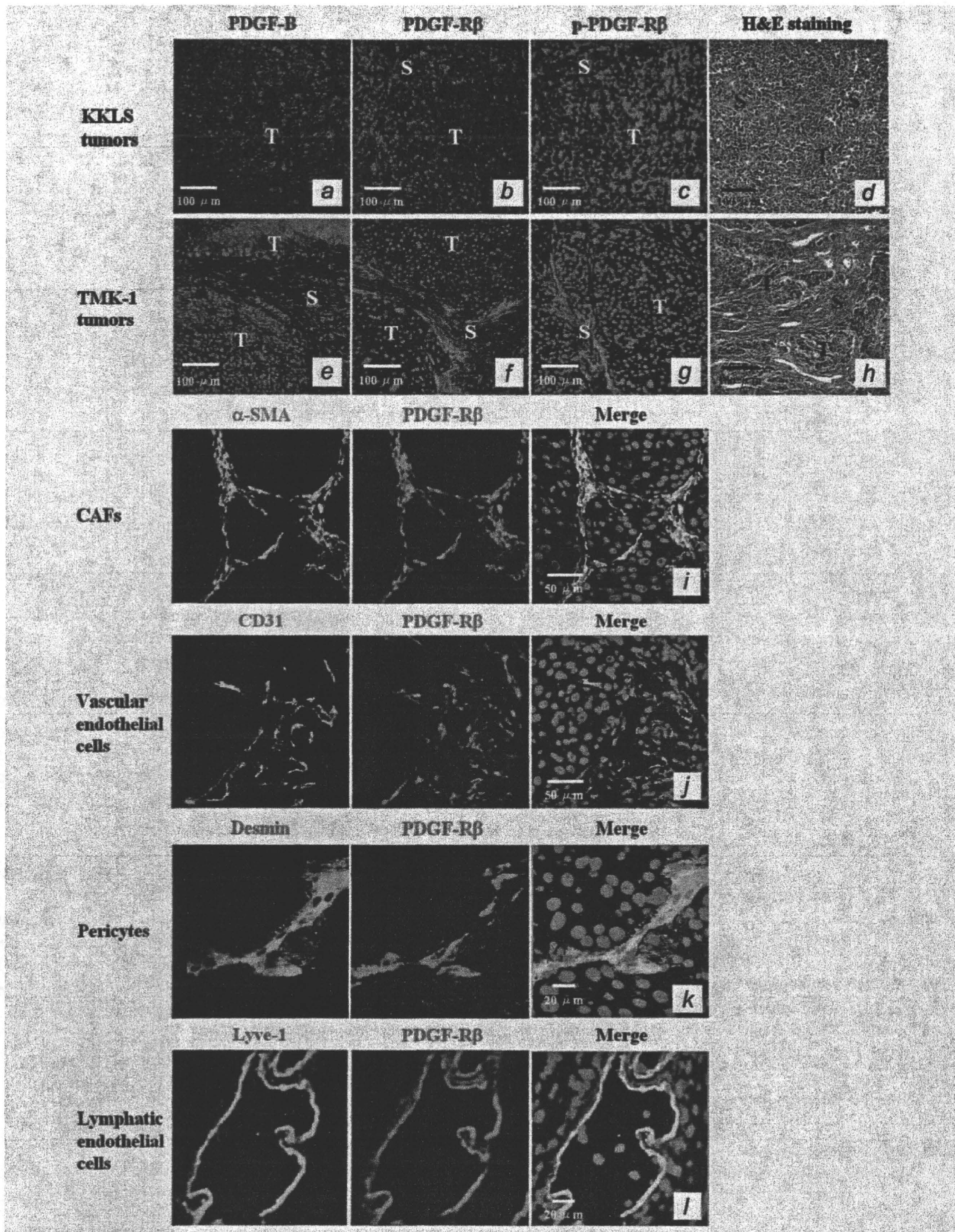

Figure 2. Hematoxylin and eosin (H&E) and immunofluorescence staining for PDGF-BB, PDGF-Rβ and p-PDGF-Rβ in KKLS and TMK-1 gastric carcinoma cells (*a–h*). Tumor cells stained positively for PDGF-B (*a* and *e*), whereas stromal cells stained positively for PDGF-Rβ (*b* and *f*). PDGF-Rβ was phosphorylated in TMK-1 tumors, but not in KKLS tumors (*c* and *g*) (red fluorescence). T, tumor nest; S, stroma. Double immunofluorescence staining for PDGF-Rβ and α-SMA (*i*), CD31 (*j*), desmin (*k*) and Lyve-1 (*l*). PDGF-Rβ-positive cells displayed red fluorescence, and α-SMA-, CD31-, desmin- and Lyve-1-positive cells displayed green fluorescence. Co-localization cells yielded yellow images.

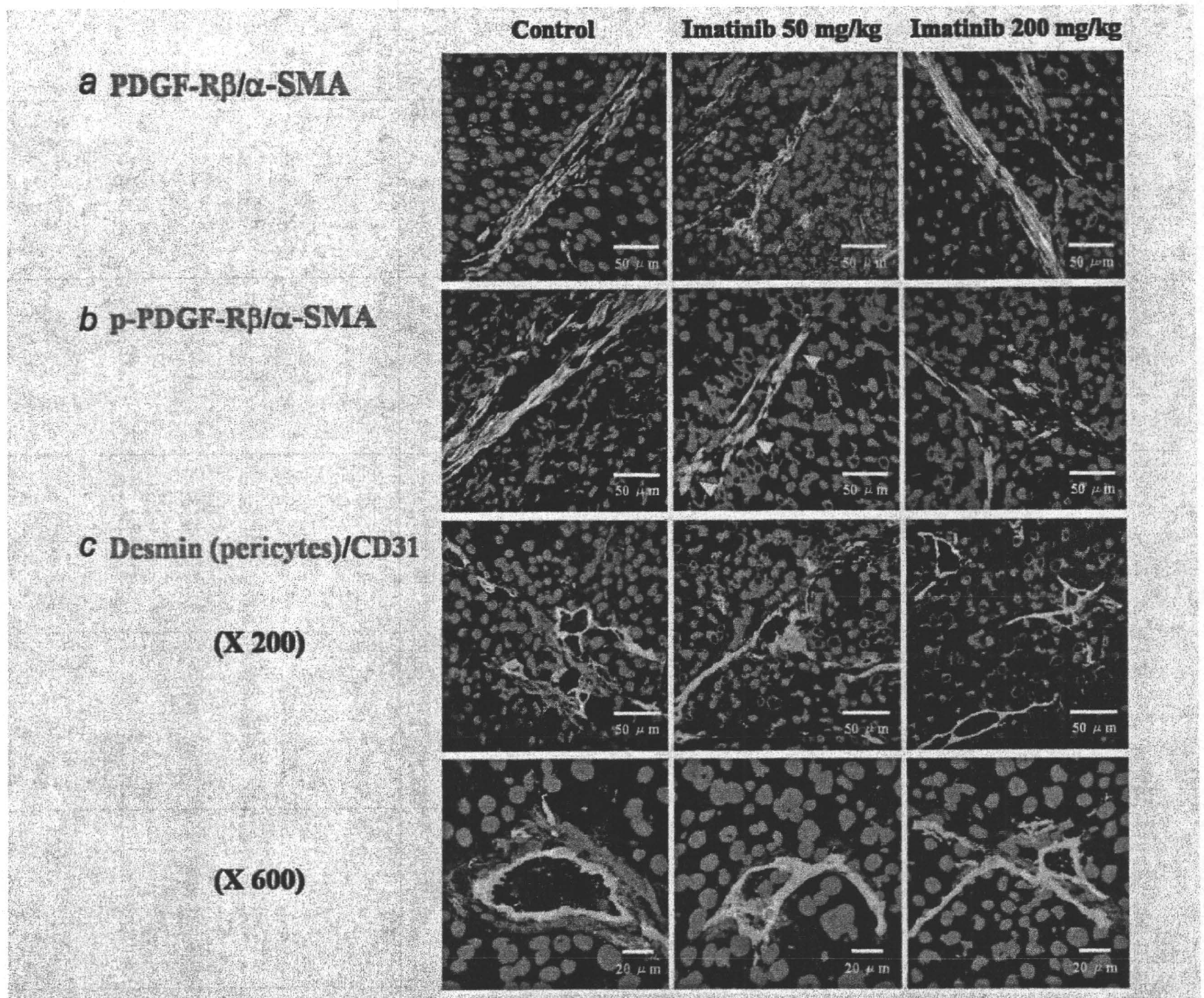

Figure 3. Effects of imatinib on carcinoma-associated fibroblasts (CAFs) and pericytes. Expression of PDGF-Rβ in CAFs did not change with treatment (*a*). Phosphorylation of PDGF-Rβ in CAFs was inhibited by treatment with imatinib. With low-dose (50 mg/kg/day) imatinib treatment, p-PDGF-Rβ expression was not completely inhibited (yellow arrowhead), but the inhibition was marked with high-dose (200 mg/kg/day) imatinib treatment (*b*). Endothelial cells were identified by green fluorescence, whereas pericytes were identified by red fluorescence (*c*). Morphological findings and the distribution of pericytes differed between control and imatinib treatment groups.

combination did not significantly affect body weights (Table 1). Tumor growth and metastasis were not inhibited in mice treated with imatinib alone (*vs.* control mice); however, tumor growth was significantly inhibited in mice treated with irinotecan alone or irinotecan combined with imatinib. Mice treated with high-dose imatinib and irinotecan in combination also had significantly smaller tumors than those in mice treated with irinotecan alone (Fig. 5*a*) or with low-dose imatinib in combination with irinotecan. Lymph node and peritoneal metastasis were inhibited only in the mice treated with high-dose imatinib and irinotecan in combination (Table 1).

For comparison, we evaluated the effects of imatinib on the growth of KKLS orthotopic tumors, for which the stromal reaction is minimal, with its effects on stromal compartment-rich TMK-1 tumors. Tumor growth was not inhibited in mice treated with imatinib alone. Although tumor growth was significantly inhibited in mice treated with irinotecan alone, high-dose imatinib used in combination with irinotecan did not enhance the antitumor effects of irinotecan (Fig. 5*b*).

Histopathologic analysis of TMK-1 tumors

In control and irinotecan-treated mice, TMK-1 gastric tumors showed abundant CAFs and ECM containing Type-1 collagen. In contrast, gastric tumors in mice treated with imatinib alone or with imatinib and irinotecan in combination were

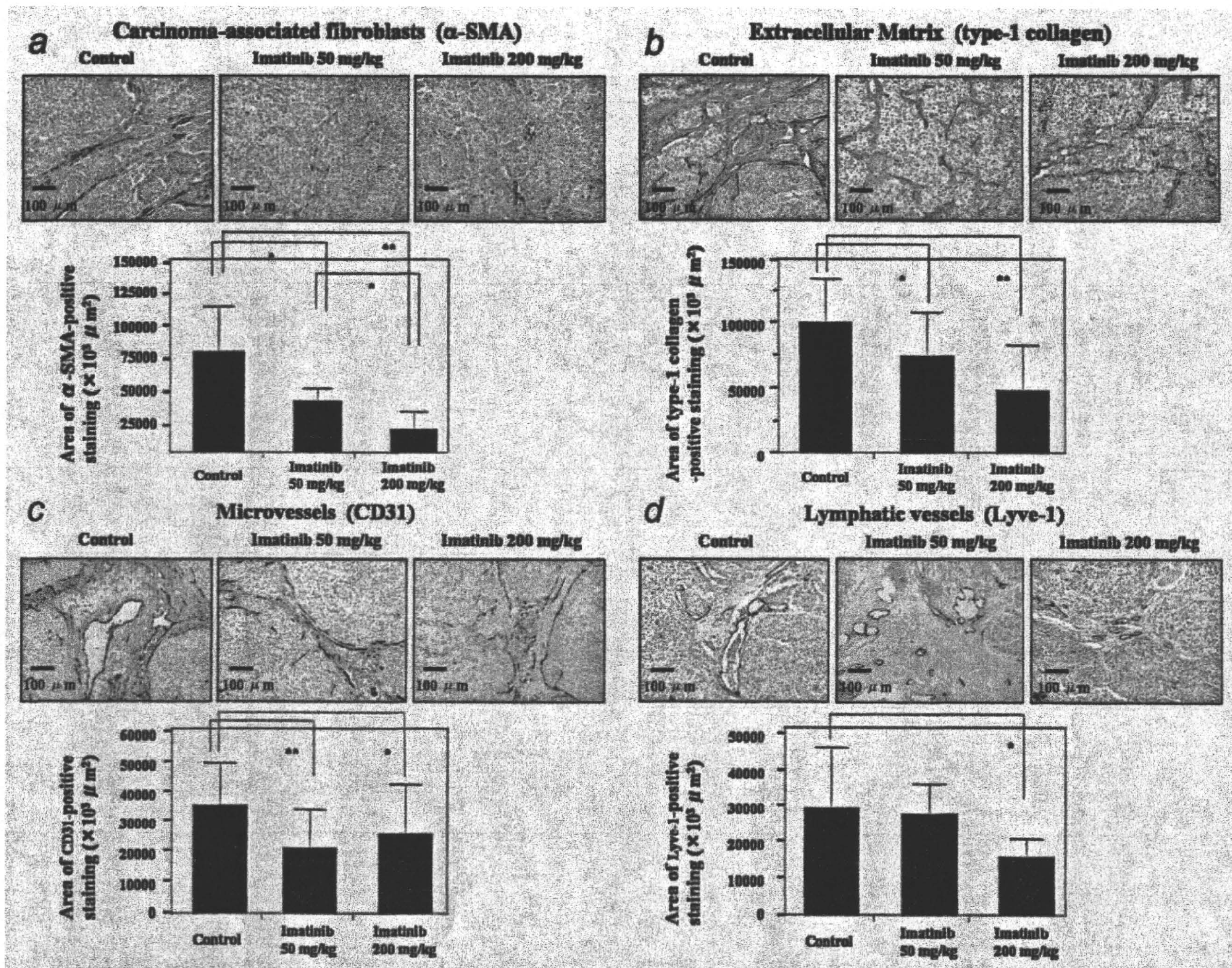

Figure 4. Dose-effects of imatinib on CAFs, extracellular matrix (ECM), vascular microvessels and lymphatic vessels were evaluated immunohistochemically according to the area of α-SMA (*a*), Type-1 collagen (*b*), CD31-positive (*c*) and Lyve-1-positive (*d*) cells, respectively. The areas of CAFs, ECM and vascular microvessels were reduced by treatment with imatinib. A reduction in the lymphatic area was observed only with high-dose imatinib treatment. *, $p < 0.05$, **, $p < 0.01$; bars, SE. [Color figure can be viewed in the online issue, which is available at wileyonlinelibrary.com.]

surrounded by scanty stroma (area of α-SMA-positive or Type-1 collagen-positive staining) (Fig. 6).

In addition, treatment with imatinib alone or with imatinib and irinotecan in combination significantly reduced the areas of vascular microvessels and lymphatic vessels as well as the number of pericytes (Table 2).

Proliferation of tumor cells was evaluated by staining for Ki-67. The control group Ki-67 LI was 57.3 ± 15.0. As shown in Table 2, the Ki-67 LI was significantly decreased after treatment with high-dose imatinib alone (41.7 ± 6.74, $p < 0.05$) or with irinotecan alone (37.7 ± 21.1, $p < 0.05$) and also after treatment with the two drugs in combination (39.7 ± 7.85; $p < 0.01$, 28.1 ± 14.3; $p < 0.01$, respectively).

According to TUNEL assay, the median number of apoptotic tumor cells in control mice was 5.54 ± 1.64. The number of apoptotic cells in tumors of mice from each of the treatment groups did not differ significantly from the number in control mice (Table 2).

Discussion

In our orthotopic nude mouse model of human gastric carcinoma, we found that blockade of PDGF-Rβ signaling by oral administration of PDGF-R tyrosine kinase inhibitor imatinib combined with intraperitoneal injection of irinotecan significantly inhibited not only the growth of tumors but also the incidences of lymph node and peritoneal metastasis. PDGF production and autocrine stimulation of cancer growth are described for only a subset of cancer types, *e.g.*, glioblastomas and sarcomas.[33,34] Most cancer cells, as secreting PDGF ligands, do not express PDGF-Rs, suggesting that PDGF may act as a paracrine growth factor.[35,36] In our experiments, PDGF-B was expressed by TMK-1 gastric carcinoma cells, whereas PDGF-

Table 1. Antitumor effects of imatinib and irinotecan in TMK-1 gastric carcinoma cells

Treatment group	Body weight (g)	Tumor incidence	Tumor weight (g)	Lymph node metastasis	Peritoneal metastasis	Liver metastasis
Control	21.8 (17.5–25.2)	10/10	3.13 (2.40–3.89)	8/10	6/10	1/10
Imatinib (50 mg/kg)	20.6 (17.2–22.7)	10/10	3.34 (1.92–4.50)	7/10	3/10	0/10
Imatinib (200 mg/kg)	22.0 (19.5–24.3)	9/9	2.26 (0.68–5.50)	6/9	3/9	2/9
Irinotecan (5 mg/kg)	21.3 (19.1–25.2)	10/10	1.33 (0.66–2.16)**	5/10	5/10	2/10
Irinotecan (5 mg/kg) + imatinib (50 mg/kg)	19.0 (16.1–21.4)	9/9	1.11 (0.53–1.80)**	7/9	3/9	1/9
Irinotecan (5 mg/kg) + imatinib (200 mg/kg)	21.8 (19.1–24.5)	9/9	0.59 (0.32–1.01)**	2/9*	1/9*	0/9

TMK-1 cells (1×10^6) were injected into the gastric wall of nude mice. Two weeks later, the mice were randomly assigned to receive water daily by oral gavage and intraperitoneal injection of PBS once per week (control); oral gavage of imatinib (50 mg/kg or 200 mg/kg) daily and weekly intraperitoneal injection of PBS; irinotecan intraperitoneally once per week and daily administration of water by oral gavage; or oral gavage of imatinib (50 mg/kg or 200 mg/kg) daily and weekly intraperitoneal injection of irinotecan. Treatments continued for 28 days. Number of individual mice is shown unless otherwise indicated. Ranges are shown in parentheses.
$^*p < 0.05$ *vs.* control group, values. $^{**}p < 0.01$ *vs.* control group, values.

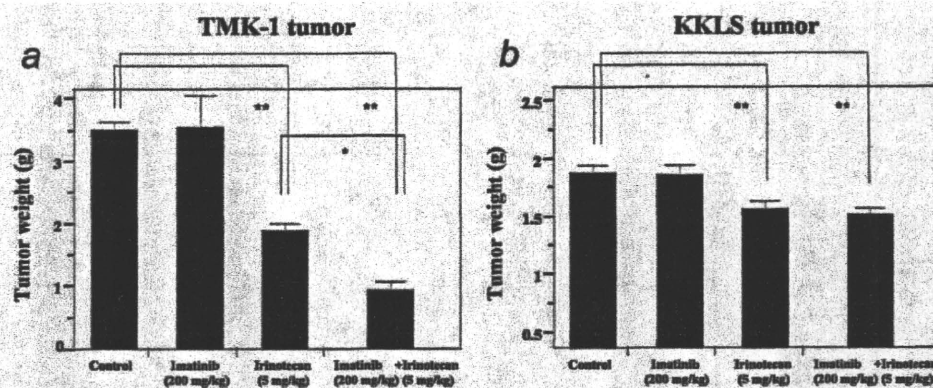

Figure 5. Antitumor effects of imatinib and irinotecan on the growth of TMK-1 and KKLS orthotopic tumors. In TMK-1 tumors, tumor growth was significantly inhibited in mice treated with irinotecan alone and imatinib in combination with irinotecan enhanced the antitumor effects of irinotecan (*a*). In contrast, imatinib did not enhance the antitumor effects of irinotecan in KKLS tumors (*b*). *, $p < 0.01$, **, $p < 0.001$; bars, SE.

Rβ was expressed mainly by stromal cells, including CAFs, pericytes and lymphatic endothelial cells. Blockade of PDGF-R signaling decreased stromal reaction, areas of vascular and lymphatic vessels and number of pericytes.

Kim *et al.* reported that inhibition of PDGF-R by imatinib enhanced the effect of chemotherapeutic reagents; however, they used an ectopic (subcutaneous) model of gastric carcinoma.[37] The organ microenvironment is known to influence the growth, vascularization, invasion and, hence, metastasis of human neoplasms.[38] Because ectopic tumors generally do not metastasize, the metastatic ability of tumor cells cannot be evaluated in an ectopic transplantation model. In addition, we reported previously that the expression of PDGF-Rβ by stromal cells in a colon cancer model was higher in tumors growing at the orthotopic site than in those growing at the ectopic site.[39] In the orthotopic site (cecal wall), the tumors induced a strong stromal reaction, whereas in the subcutis, the stromal reaction was minimal.[39] Treatment with imatinib and irinotecan significantly inhibited tumor growth in the cecum but not in the subcutis.[25] Thus, orthotopic transplantation models should be used in experimental studies to evaluate the inhibitory effect of therapeutic agents on metastasis.[38]

Recent studies have shown that tumor growth is determined not only by malignant cancer cells themselves but also by the tumor stroma.[40] Tumor stroma consists of CAFs, smooth muscle cells, inflammatory cells, microvessels and abundant ECM.[41] CAFs synthesize many of the constituents of fibrillar ECM, such as Type-I, Type-III and Type-V collagen and fibronectin.[42,43] CAFs are known to modulate tumorigenic properties of neoplastic cells, including proliferation, apoptosis and angiogenesis,[44] and they are thought to play a central role in the complex process of tumor-stroma interaction and consequent-tumorigenesis.[36] Experiments involving coinjection of CAFs and tumor cells have shown that, in contrast to normal fibroblasts, CAFs promote tumor growth.[45] Moreover, recent studies have revealed extensive

Table 2. Immunohistochemical analysis of TMK-1 human gastric carcinoma cells

Treatment group	Tumor cells		Tumor-associated endothelial cells		Lymphatic endothelial cells
	Ki-67 LI[1] (%)	TUNEL[2] (%)	MVA[3] (/× 10^3 μm^2)	Pericyte coverage[4] (%)	LVA[5] (/× 10^3 μm^2)
Control	57.3 ± 15.0	5.54 ± 1.64	38.6 ± 4.75	56.8 ± 4.65	27.8 ± 5.28
Imatinib (50 mg/kg)	50.7 ± 9.97	5.96 ± 2.45	22.2 ± 4.55**	31.5 ± 3.34*	27.0 ± 2.73
Imatinib (200 mg/kg)	41.7 ± 6.74*	4.74 ± 0.55	27.7 ± 5.34*	22.1 ± 6.16*	14.9 ± 1.51*
Irinotecan (5 mg/kg)	37.7 ± 21.1*	4.54 ± 0.36	40.8 ± 12.6	63.7 ± 10.5	21.5 ± 1.83
Irinotecan (5 mg/kg) + imatinib (50 mg/kg)	39.7 ± 7.85**	5.19 ± 1.22	26.6 ± 0.87*	45.5 ± 4.44*	20.8 ± 1.64
Irinotecan (5 mg/kg) + imatinib (200 mg/kg)	28.1 ± 14.3**	6.23 ± 3.12	18.8 ± 3.36**	10.1 ± 2.04*	16.1 ± 2.43*

[1]Number (mean ± SE) of Ki-67-positive tumor cells/field determined by measuring 10 random 0.81-mm^2 fields at 100× magnification. [2]Percentage of TUNEL-positive tumor cells (out of total number of cells) per 0.81-mm^2 fields at 100× magnification. [3]MVA was determined by measuring 10 random fields at 100× magnification. [4]LVA was determined by measuring 10 random fields at 100× magnification. [5]CD31-positive cells in direct contact with desmin-positive cells were counted in five random fields at 100× magnification. *$p < 0.05$ *vs.* control group, values. **$p < 0.01$ *vs.* control group, values.
Abbreviations: Ki-67 LI: Ki-67 labeling index; MVA: microvessel area; LVA: lymphatic vessel area.

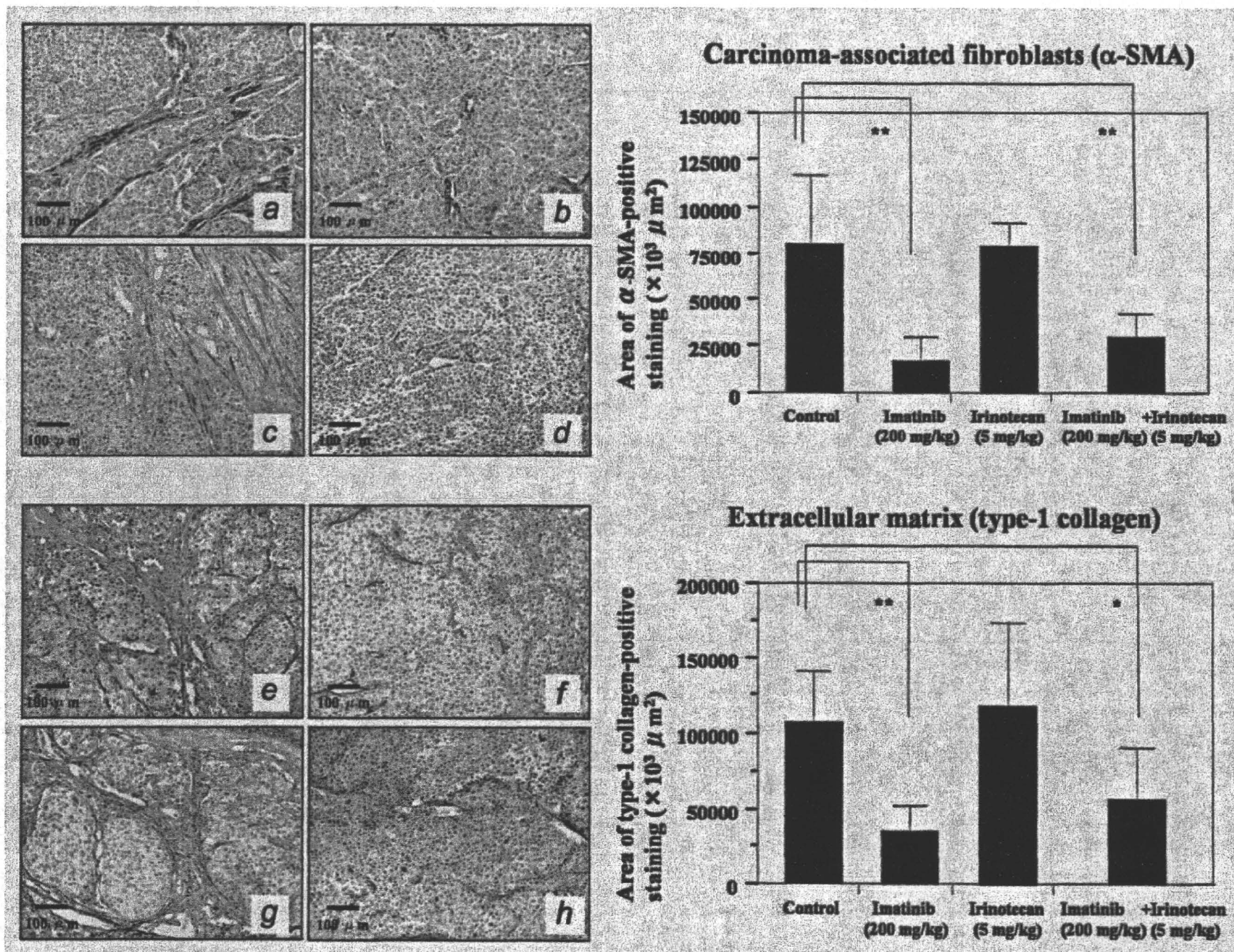

Figure 6. CAFs and ECM were quantified according to the α-SMA-positive (*a–d*) and Type-1 collagen-positive (*e–h*) areas. The areas of CAFs and ECM were reduced with treatment with imatinib alone and imatinib in combination with irinotecan. (*a* and *e*): control; (*b* and *f*): imatinib (200 mg/kg); (*c* and *g*): irinotecan (5 mg/kg); (*d* and *h*): imatinib (200 mg/kg) plus irinotecan (5 mg/kg). *, $p < 0.05$, **, $p < 0.01$; bars, SE. [Color figure can be viewed in the online issue, which is available at wileyonlinelibrary.com.]

changes in the phenotype, and even the genotype, of CAFs compared with their normal counterparts.[46] Lieubeau *et al.* reported that progressive tumor growth correlates with proliferation of myofibroblasts, whereas regression of tumors is linked to the fibrous capsule, suggesting that the presence of reactive stromal cells (myofibroblasts) may contribute to the growth of tumor cells.[47] Other studies have shown that a poor prognosis in cases of colorectal carcinoma is associated with abundance of CAFs or increased expression of fibroblast-activated protein.[48,49] It has also been shown that CAFs can affect sensitivity of pancreatic carcinoma cells to chemo- or radio-therapy; such tumor cells become less sensitive to chemotherapy when co-cultured with CAFs or grown in fibroblast-conditioned medium.[50] Therefore, CAFs are considered novel targets for anti-tumor therapies.

Increased IFP in solid tumors, which is mediated by an increase in stromal compartment pressure, acts as a barrier between tumor cells and normal tissues against effective distribution of anti-tumor drugs. It has also been reported that increased IFP prevents tumor transvascular transport of effector cells.[51] The PDGF/PDGF-R signaling pathway plays a critical role in the control of IFP.[24,51] A number of studies have shown that inhibition of PDGF-R signaling can decrease this pressure and, hence, enhance the effects chemotherapeutic reagents.[14] In our TMK-1 model, we observed that inhibition of tumor growth and metastasis by combination imatinib and irinotecan treatment was associated with the reduction in CAFs and ECM, suggesting that similar mechanisms may be involved in gastric carcinoma.

Treatment with imatinib influences microvessel structure in tumor tissues. Pericytes in tumor-associated vessels, but not those in vessels of normal mucosa, are enlarged and they overexpress PDGF-Rβ and p-PDGF-Rβ.[39] In agreement with earlier reports,[13,31] treatment with imatinib decreased pericyte coverage on tumor-associated endothelial cells in our experimental model. The inhibition of PDGF-R signaling may decrease pericyte recruitment and attachment to endothelial cells and destabilize the tumor vasculature.

VEGF-C and -D are well-known lymphangiogenic factors in human gastric carcinoma. Other growth factors recently reported to be lymphangiogenic are FGF-2,[52] PDGF-BB[53] and angiopoietin-2.[54] In this study, we showed that lymphatic endothelial cells express PDGF-R and that inhibition of PDGFR results in a reduction of the lymphatic vessel area. We recently found correlation between the level of PDGF-B mRNA expression in gastric carcinoma tissue and lymphatic metastasis.[55] These findings suggest that PDGF-B acts as a lymphangiogenic factor. However, it is a possible that treatment with imatinib exerts indirect anti-lymphangiogenic effects *via* inhibition of VEGF-C and -D production by tumor cells and/or stromal cells. In addition, imatinib at a high concentration can block various tyrosine kinases to different extents. Molecules other than PDGF-Rs may be involved in the regulation of lymphangiogenesis. Further studies are needed to confirm whether the PDGF/PDGF-R axis is directly involved in lymphangiogenesis in gastric carcinoma.

In summary, targeting stromal cells by PDGF-R inhibitor appears promising as a therapeutic strategy against carcinoma. Stromal compartment-rich tumors, such as diffuse-type gastric carcinomas, may be tumors in which targeting the PDGF/PDGF-R signaling pathway for enhancement of the chemotherapeutic effect is most applicable.

Acknowledgements

This work was carried out with the kind cooperation of the Analysis Center of Life Science and Institute of Laboratory Animal Science, Hiroshima University, Hiroshima, Japan, and we thank Novartis Pharma K.K. (Basal, Switzerland) for providing the imatinib.

References

1. Mantovani A, Allavena P, Sica A, Balkwill F. Cancer-related inflammation. *Nature* 2008;454:436–44.
2. Whiteside TL. The tumor microenvironment and its role in promoting tumor growth. *Oncogene* 2008; 27:5904–12.
3. Mueller MM, Fusenig NE. Friends or foes—bipolar effects of the tumour stroma in cancer. *Nat Rev Cancer* 2004;4:839–49.
4. Kitadai Y. Cancer-stromal cell interaction and tumor angiogenesis in gastric cancer. *Cancer Microenviron*, 2010;3:109–16.
5. Uehara H, Kim SJ, Karashima T, Shepherd DL, Fan D, Tsan R, Killion JJ, Logothetis C, Mathew P, Fidler IJ. Effects of blocking platelet-derived growth factor-receptor signaling in a mouse model of experimental prostate cancer bone metastases. *J Natl Cancer Inst* 2003;95: 458–70.
6. Antoniades HN, Galanopoulos T, Neville-Golden J, O'Hara CJ. Malignant epithelial cells in primary human lung carcinomas coexpress in vivo platelet-derived growth factor (PDGF) and PDGF receptor mRNAs and their protein products. *Proc Natl Acad Sci USA* 1992;89:3942–6.
7. Lindmark G, Sundberg C, Glimelius B, Pahlman L, Rubin K, Gerdin B. Stromal expression of platelet-derived growth factor beta-receptor and platelet-derived growth factor B-chain in colorectal cancer. *Lab Invest* 1993;69:682–9.
8. Seymour L, Dajee D, Bezwoda WR. Tissue platelet derived-growth factor (PDGF) predicts for shortened survival and treatment failure in advanced breast cancer. *Breast Cancer Res Treat* 1993;26: 247–52.
9. Yi B, Williams PJ, Niewolna M, Wang Y, Yoneda T. Tumor-derived platelet-derived growth factor-BB plays a critical role in osteosclerotic bone metastasis in an animal model of human breast cancer. *Cancer Res* 2002;62:917–23.
10. Bergsten E, Uutela M, Li X, Pietras K, Ostman A, Heldin CH, Alitalo K, Eriksson U. PDGF-D is a specific, protease-activated ligand for the PDGF beta-receptor. *Nat Cell Biol* 2001;3:512–16.
11. Ostman A. PDGF receptors-mediators of autocrine tumor growth and regulators of tumor vasculature and stroma. *Cytokine Growth Factor Rev* 2004;15: 275–86.
12. Risau W, Drexler H, Mironov V, Smits A, Siegbahn A, Funa K, Heldin CH. Platelet-derived growth factor is angiogenic in vivo. *Growth Factors* 1992;7:261–6.
13. Bergers G, Song S, Meyer-Morse N, Bergsland E, Hanahan D. Benefits of targeting both pericytes and endothelial

cells in the tumor vasculature with kinase inhibitors. *J Clin Invest* 2003;111:1287–95.
14. Pietras K. Increasing tumor uptake of anticancer drugs with imatinib. *Semin Oncol* 2004;31 (Suppl 6):18–23.
15. Druker BJ, Lydon NB. Lessons learned from the development of an abl tyrosine kinase inhibitor for chronic myelogenous leukemia. *J Clin Invest* 2000;105:3–7.
16. Fletcher JA. Role of KIT and platelet-derived growth factor receptors as oncoproteins. *Semin Oncol* 2004;31 (Suppl 6):4–11.
17. Day E, Waters B, Spiegel K, Alnadaf T, Manley PW, Buchdunger E, Walker C, Jarai G. Inhibition of collagen-induced discoidin domain receptor 1 and 2 activation by imatinib, nilotinib and dasatinib. *Eur J Pharmacol* 2008;599:44–53.
18. Heinrich MC, Blanke CD, Druker BJ, Corless CL. Inhibition of KIT tyrosine kinase activity: a novel molecular approach to the treatment of KIT-positive malignancies. *J Clin Oncol* 2002;20: 1692–703.
19. Beppu K, Jaboine J, Merchant MS, Mackall CL, Thiele CJ. Effect of imatinib mesylate on neuroblastoma tumorigenesis and vascular endothelial growth factor expression. *J Natl Cancer Inst* 2004;96: 46–55.
20. Kilic T, Alberta JA, Zdunek PR, Acar M, Iannarelli P, O'Reilly T, Buchdunger E, Black PM, Stiles CD. Intracranial inhibition of platelet-derived growth factor-mediated glioblastoma cell growth by an orally active kinase inhibitor of the 2-phenylaminopyrimidine class. *Cancer Res* 2000;60:5143–50.
21. Krystal GW, Honsawek S, Litz J, Buchdunger E. The selective tyrosine kinase inhibitor STI571 inhibits small cell lung cancer growth. *Clin Cancer Res* 2000; 6:3319–26.
22. Merchant MS, Woo CW, Mackall CL, Thiele CJ. Potential use of imatinib in Ewing's sarcoma: evidence for in vitro and in vivo activity. *J Natl Cancer Inst* 2002;94: 1673–9.
23. Sjöblom T, Shimizu A, O'Brien KP, Pietras K, Dal Cin P, Buchdunger E, Dumanski JP, Ostman A, Heldin CH. Growth inhibition of dermatofibrosarcoma protuberans tumors by the platelet-derived growth factor receptor antagonist STI571 through induction of apoptosis. *Cancer Res* 2001;61: 5778–83.
24. Hwang RF, Yokoi K, Bucana CD, Tsan R, Killion JJ, Evans DB, Fidler IJ. Inhibition of platelet-derived growth factor receptor phosphorylation by STI571 (Gleevec) reduces growth and metastasis of human pancreatic carcinoma in an orthotopic nude mouse model. *Clin Cancer Res* 2003; 9:6534–44.
25. Kitadai Y, Sasaki T, Kuwai T, Nakamura T, Bucana CD, Fidler IJ. Targeting the expression of platelet-derived growth factor receptor by reactive stroma inhibits growth and metastasis of human colon carcinoma. *Am J Pathol* 2006;169:2054–65.
26. Pietras K, Pahler J, Bergers G, Hanahan D. Functions of paracrine PDGF signaling in the proangiogenic tumor stroma revealed by pharmacological targeting. *PLoS Med* 2008;5:123–38.
27. Farhat FS. A general review of the role of irinotecan (CPT11) in the treatment of gastric cancer. *Med Oncol* 2007;24:137–46.
28. Apte SM, Fan D, Killion JJ, Fidler IJ. Targeting the platelet-derived growth factor receptor in antivascular therapy for human ovarian carcinoma. *Clin Cancer Res* 2004; 10:897–908.
29. Kobie K, Kawabata M, Hioki K, Tanaka A, Matsuda H, Mori T, Maruo K. The tyrosine kinase inhibitor imatinib [STI571] induces regression of xenografted canine mast cell tumors in SCID mice. *Res Vet Sci* 2007;82:239–41.
30. Wolff NC, Veach DR, Tong WP, Bornmann WG, Clarkson B, Ilaria RL, Jr. PD166326, a novel tyrosine kinase inhibitor, has greater antileukemic activity than imatinib mesylate in a murine model of chronic myeloid leukemia. *Blood* 2005; 105:3995–4003.
31. Yokoi K, Sasaki T, Bucana CD, Fan D, Baker CH, Kitadai Y, Kuwai T, Abbruzzese JL, Fidler IJ. Simultaneous inhibition of EGFR, VEGFR, and platelet-derived growth factor receptor signaling combined with gemcitabine produces therapy of human pancreatic carcinoma and prolongs survival in an orthotopic nude mouse model. *Cancer Res* 2005;65:10371–80.
32. Peng B, Hayes M, Resta D, Racine-Poon A, Druker BJ, Talpaz M, Sawyers CL, Rosamilia M, Ford J, Lloyd P, Capdeville R. Pharmacokinetics and pharmacodynamics of imatinib in a phase I trial with chronic myeloid leukemia patients. *J Clin Oncol* 2004;22:935–42.
33. Hermanson M, Funa K, Hartman M, Claesson-Welsh L, Heldin CH, Westermark B, Nistér M. Platelet-derived growth factor and its receptors in human glioma tissue: expression of messenger RNA and protein suggests the presence of autocrine and paracrine loops. *Cancer Res* 1992;52: 3213–19.
34. Smits A, Funa K, Vassbotn FS, Beausang-Linder M, af Ekenstam F, Heldin CH, Westermark B, Nister M. Expression of platelet-derived growth factor and its receptors in proliferative disorders of fibroblastic origin. *Am J Pathol* 1992;140: 639–48.
35. Forsberg K, Valyi-Nagy I, Heldin CH, Herlyn M, Westermark B. Platelet-derived growth factor (PDGF) in oncogenesis: development of a vascular connective tissue stroma in xenotransplanted human melanoma producing PDGF-BB. *Proc Natl Acad Sci USA* 1993;90:393–7.
36. Micke P, Ostman A. Tumour-stroma interaction: cancer-associated fibroblasts as novel targets in anti-cancer therapy? *Lung Cancer* 2004;45 (Suppl 2): S163–S175.
37. Kim R, Emi M, Arihiro K, Tanabe K, Uchida Y, Toge T. Chemosensitization by STI571 targeting the platelet-derived growth factor/platelet-derived growth factor receptor-signaling pathway in the tumor progression and angiogenesis of gastric carcinoma. *Cancer* 2005;103:1800–9.
38. Fidler IJ, Wilmanns C, Staroselsky A, Radinsky R, Dong Z, Fan D. Modulation of tumor cell response to chemotherapy by the organ environment. *Cancer Metastasis Rev* 1994;13:209–22.
39. Kitadai Y, Sasaki T, Kuwai T, Nakamura T, Bucana CD, Hamilton SR, Fidler IJ. Expression of activated platelet-derived growth factor receptor in stromal cells of human colon carcinomas is associated with metastatic potential. *Int J Cancer* 2006;119: 2567–74.
40. Kalluri R. Basement membranes: structure, assembly and role in tumour angiogenesis. *Nat Rev Cancer* 2003;3:422–33.
41. Hanahan D, Weinberg RA. The hallmarks of cancer. *Cell* 2000;100:57–70.
42. Rodemann HP, Muller GA. Characterization of human renal fibroblasts in health and disease. II. In vitro growth, differentiation, and collagen synthesis of fibroblasts from kidneys with interstitial fibrosis. *Am J Kidney Dis* 1991;17:684–6.
43. Tomasek JJ, Gabbiani G, Hinz B, Chaponnier C, Brown RA. Myofibroblasts and mechano-regulation of connective tissue remodelling. *Nat Rev Mol Cell Biol* 2002;3:349–63.
44. Micke P, Ostman A. Exploring the tumour environment: cancer-associated fibroblasts as targets in cancer therapy. *Expert Opin Ther Targets* 2005;9:1217–33.
45. Tuxhorn JA, Ayala GE, Rowley DR. Reactive stroma in prostate cancer progression. *J Urol* 2001;166:2472–83.
46. Moinfar F, Man YG, Arnould L, Bratthauer GL, Ratschek M, Tavassoli FA. Concurrent and independent genetic alterations in the stromal and epithelial cells of mammary carcinoma: implications for tumorigenesis. *Cancer Res* 2000;60: 2562–6.
47. Lieubeau B, Garrigue L, Barbieux I, Meflah K, Gregoire M. The role of transforming growth factor beta 1 in the fibroblastic reaction associated with rat colorectal tumor development. *Cancer Res* 1994;54: 6526–32.

48. Henry LR, Lee HO, Lee JS, Klein-Szanto A, Watts P, Ross EA, Chen WT, Cheng JD. Clinical implications of fibroblast activation protein in patients with colon cancer. *Clin Cancer Res* 2007; 13:1736–41.
49. Tsujino T, Seshimo I, Yamamoto H, Ngan CY, Ezumi K, Takemasa I, Ikeda M, Sekimoto M, Matsuura N, Monden M. Stromal myofibroblasts predict disease recurrence for colorectal cancer. *Clin Cancer Res* 2007;13:2082–90.
50. Hwang RF, Moore T, Arumugam T, Ramachandran V, Amos KD, Rivera A, Ji B, Evans DB, Logsdon CD. Cancer-associated stromal fibroblasts promote pancreatic tumor progression. *Cancer Res* 2008;68:918–26.
51. Pietras K, Ostman A, Sjoquist M, Buchdunger E, Reed RK, Heldin CH, Rubin K. Inhibition of platelet-derived growth factor receptors reduces interstitial hypertension and increases transcapillary transport in tumors. *Cancer Res* 2001;61: 2929–34.
52. Kubo H, Cao R, Brakenhielm E, Makinen T, Cao Y, Alitalo K. Blockade of vascular endothelial growth factor receptor-3 signaling inhibits fibroblast growth factor-2-induced lymphangiogenesis in mouse cornea. *Proc Natl Acad Sci USA* 2002;99: 8868–73.
53. Cao R, Bjorndahl MA, Religa P, Clasper S, Garvin S, Galter D, Meister B, Ikomi F, Tritsaris K, Dissing S, Ohhashi T, Jackson DG, et al. PDGF-BB induces intratumoral lymphangiogenesis and promotes lymphatic metastasis. *Cancer Cell* 2004;6:333–45.
54. Gale NW, Thurston G, Hackett SF, Renard R, Wang Q, McClain J, Martin C, Witte C, Witte MH, Jackson D, Suri C, Campochiaro PA, et al. Angiopoietin-2 is required for postnatal angiogenesis and lymphatic patterning, and only the latter role is rescued by angiopoietin-1. *Dev Cell* 2002;3:411–23.
55. Kodama M, Kitadai Y, Sumida T, Ohnishi M, Ohara E, Tanaka M, Shinagawa K, Tanaka S, Yasui W, Chayama K. Expression of platelet-derived growth factor (PDGF)-B and PDGF-receptor beta is associated with lymphatic metastasis in human gastric carcinoma. *Cancer Sci*, 2010: 101:1984–9.

GASTROENTEROLOGY 2011;140:892–902

A Functional Single Nucleotide Polymorphism in *Mucin 1*, at Chromosome 1q22, Determines Susceptibility to Diffuse-Type Gastric Cancer

NORIHISA SAEKI,* AKIRA SAITO,*,‡ IL JU CHOI,§ KEITARO MATSUO,‖ SUMIKO OHNAMI,* HIROHIKO TOTSUKA,*,¶ SUENORI CHIKU,*,# AYA KUCHIBA,* YEON-SU LEE,§ KYONG-AH YOON,§ MYEONG-CHERL KOOK,§ SOOK RYUN PARK,§ YOUNG-WOO KIM,§ HIDEO TANAKA,‖ KAZUO TAJIMA,‖ HIROSHI HIROSE,** FUMIHIKO TANIOKA,‡‡ YOSHIHIRO MATSUNO,§§ HARUHIKO SUGIMURA,‖‖ SHUNJI KATO,¶¶ TSUNEYA NAKAMURA,## TOMOHIRO NISHINA,*** WATARU YASUI,‡‡‡ KAZUHIKO AOYAGI,* HIROKI SASAKI,* KAZUYOSHI YANAGIHARA,§§§ HITOSHI KATAI,‖‖‖ TADAKAZU SHIMODA,¶¶¶ TERUHIKO YOSHIDA,* YUSUKE NAKAMURA,###,**** SETSUO HIROHASHI,**** and HIROMI SAKAMOTO*

*Genetics Division, National Cancer Center Research Institute, Tokyo; ‡Statistical Genetics Analysis Division, StaGen Co, Ltd, Tokyo, Japan; §Research Institute and Hospital, National Cancer Center, Gyeonggi-do, Korea; ‖Division of Epidemiology and Prevention, Aichi Cancer Center Research Institute, Nagoya; ¶Bioinformatics Group, Research and Development Center, Solution Division 4, Hitachi Government and Public Corporation System Engineering Ltd, Tokyo; #Science Solutions Division, Mizuho Information and Research Institute, Inc, Tokyo; **Department of Internal Medicine, Keio University School of Medicine, Tokyo; ‡‡Iwata City Hospital, Shizuoka; §§Department of Surgical Pathology, Hokkaido University Hospital, Sapporo; ‖‖First Department of Pathology, Hamamatsu University School of Medicine, Shizuoka; ¶¶Department of Surgery, Nippon Medical School Hospital, Tokyo; ##Department of Endoscopy, Aichi Cancer Center Hospital, Nagoya; ***Department of Internal Medicine, Shikoku Cancer Center, Ehime; ‡‡‡Department of Molecular Pathology, Hiroshima University Graduate School of Biomedical Sciences, Hiroshima; §§§Department of Life Sciences, Yasuda Women's University Faculty of Pharmacy, Hiroshima; ‖‖‖Department of Surgical Oncology, National Cancer Center Hospital, Tokyo; ¶¶¶Center for Cancer Control and Information Services, National Cancer Center, Tokyo; ###Human Genome Center, Institute of Medical Science, University of Tokyo, Tokyo; and ****National Cancer Center Research Institute, Tokyo, Japan

BASIC-ALIMENTARY TRACT

BACKGROUND & AIMS: Two major types of gastric cancer, intestinal and diffuse, develop through distinct mechanisms; the diffuse type is considered to be more influenced by genetic factors, although the mechanism is unknown. Our previous genome-wide association study associated 3 single nucleotide polymorphisms (SNPs) with diffuse-type gastric cancer (DGC); 1 was a functional SNP (rs2294008) in *prostate stem cell antigen* (*PSCA*), but the loci of the other 2 were not investigated. **METHODS:** We performed high-density mapping to explore a linkage disequilibrium status of the 2 SNPs at chromosome 1q22. A DGC case-control study was conducted using DNA from 606 cases and 1264 controls (all Japanese individuals) and validated using DNA from Japanese (304 cases, 1465 controls) and Korean (452 cases, 372 controls) individuals. The effects of SNPs on function were analyzed by reporter assays and analyses of splice variants. **RESULTS:** A region of a strong linkage disequilibrium with the 2 SNPs contained *mucin 1* (*MUC1*) and other 4 genes and SNPs significantly associated with DGC (rs2070803: $P = 4.33 \times 10^{-13}$; odds ratio [OR], 1.71 by meta-analysis of the studies on the 3 panels) but not with intestinal-type gastric cancer. Functional studies demonstrated that rs4072037 ($P = 1.43 \times 10^{-11}$; OR, 1.66 by meta-analysis) in *MUC1* affects promoter activity and determines the major splicing variants of *MUC1* in the gastric epithelium. Individuals that carry both SNPs rs2294008 in *PSCA* and rs4072037 in *MUC1* have a high risk for developing DGC (OR, 8.38). **CONCLUSIONS:** ***MUC1* is the second major DGC susceptibility gene identified. The SNPs rs2070803 and rs4072037 in *MUC1* might be used to identify individuals at risk for this type of gastric cancer.**

Keywords: Stomach Cancer; Risk Genotype; Cancer Prevention; Genome-Wide Association Study.

Gastric cancer (GC) is the fourth most common cancer and the second most common cause of cancer death in the world.[1] More than 90% of GC are adenocarcinomas, which are classified into diffuse-type GC (DGC) and intestinal-type GC (IGC).[2] Typically, IGC arises through a sequence of pathologic changes of the gastric epithelium: chronic gastritis mainly because of *Helicobacter pylori* infection, atrophic gastritis, intestinal metaplasia, dysplasia, and adenocarcinoma.[3] On the other hand, the origin of DGC has been considered to be gastric epithelial stem cells and/or precursors present in the isthmus region of the middle portion of the epithelium (Supplementary Figure 1). Genetic and epigenetic events acting on the stem/precursor cells may cause a deviation from their normal differentiation program and lead to a DGC development,[4] although details are yet to be revealed. In contrast to the steady decline of the incidence of IGC, mainly because of the decreasing prevalence of *H pylori* infection, DGC appears to be increasing.[5] Moreover, some DGC develops to a highly malignant form,

Abbreviations used in this paper: DGC, diffuse-type gastric cancer; GC, gastric cancer; GWAS, genome-wide association study; IGC, intestinal-type gastric cancer; kb, kilobase; LD, linkage disequilibrium; *MUC1*, mucin 1; OR, odds ratio; por, poorly differentiated adenocarcinoma; *PSCA*, *prostate stem cell antigen*; sig, signet-ring cell carcinoma; TR, tandem repeats.

© 2011 by the AGA Institute
0016-5085/$36.00
doi:10.1053/j.gastro.2010.10.058

linitis plastica.[6] Identification of genetic predisposing factors and molecular pathways for the DGC development is one of the fundamentals for conceiving effective prevention, early diagnosis and therapeutic strategies.

Previously, we conducted a gene-centric genome-wide association study (GWAS) on DGC and identified 3 statistically significant single nucleotide polymorphisms (SNPs) at 2 loci after Bonferroni correction ($P < 1.8 \times 10^{-5}$) in the second stage of the screening.[7] Of the 3 SNPs, rs2976392 showed the lowest *P* value and tagged a linkage disequilibrium (LD) block at chromosome 8q24.3, in which we identified *prostate stem cell antigen* (*PSCA*) encoding prostate stem cell antigen as the novel DGC susceptibility gene. In the present study, we investigated the second genomic region of interest at chromosome 1q22, which harbors the remaining 2 SNPs, rs2075570 and rs2070803,[7] and identified *mucin 1* (*MUC1*) as the possible causal gene of the association of the region to DGC. The association between the gene and GC had been suggested also in previous reports.[8-11] However, unlike the previous candidate gene approach, we have reached the gene by performing a hypothesis-free GWAS followed by biologic studies in which a rationale of the association was obtained through the analyses of the function of a SNP rs4072037. Moreover, this study has a sufficient power as a systematic survey of genetic factors with the expected range of effect size and allele frequencies, generating a convincing level of statistical association ($P < 10^{-10}$ as compared with $P \sim 10^{-2}$ by the previous candidate gene approach[11]). The SNP rs4072037 is known to determine a splicing acceptor site in the second exon of *MUC1*.[12] In this study, we showed that the SNP is also related to major splicing variant selection in the stomach and has effect on the *MUC1* promoter activity, both of which may result in MUC1 functional difference between the individuals.

Materials and Methods

Samples

In Japan, the common type of GC is classified into 7 categories: papillary adenocarcinoma (pap), tubular adenocarcinoma (tub1 and tub2), poorly differentiated adenocarcinoma (por1 and por2), signet-ring cell carcinoma (sig), and mucinous adenocarcinoma (muc). However, a classification into 2 major categories by Lauren,[2] intestinal and diffuse types, is used worldwide especially for clinicoepidemiologic studies. A review of the classification systems is described elsewhere.[7] Basically, the DGC under the Lauren classification corresponds to por2 (nonsolid type) of poorly differentiated adenocarcinoma and sig by Japanese classification, although some investigators consider that por1 (solid type) is also included in DGC.[13]

Details of DNA samples used in the SNP typing and the association study of the chromosome 1q22 locus are as follows: In the Tokyo data set study, 610 DNA samples from patients with DGC (320 males; mean age, 55.4; 290 females; mean age, 54.0) were prepared either from methanol-fixed, paraffin-embedded tissues of noncancerous gastric mucosa or lymph nodes, or from peripheral blood, of patients with either the linitis plastica type of GC or early-stage cancer diagnosed as macroscopic type 0 IIc with histologic type of por2 and/or sig. The DGC samples in the Tokyo data set were collected at 4 institutions: the National Cancer Center Hospital in Tokyo: 360 paraffin-embedded tissues and 164 blood samples; Nippon Medical School Hospital in Tokyo: 76 blood samples; Aichi Cancer Center in Aichi: 1 blood sample; and Shikoku Cancer Center in Ehime: 9 blood samples. The control DNA samples were from peripheral blood leukocytes of 1266 volunteer individuals (male, 849; mean age, 67.2; female, 417; mean age, 59.8) with no known malignancies, who offered blood at a health check examination at Iwata City Hospital in Shizuoka and at Keio University campuses in Tokyo.

In the Aichi data set study, the DGC case samples were obtained from peripheral blood of 304 patients with histologic diagnosis of por1, por2, or sig (199 males; mean age, 57.3; 105 females; mean age, 56.4). Control blood samples were from 1467 volunteer individuals (1098 males; mean age, 59.8; 369 females; mean age, 57.3) with no known malignancies. Power calculations for the DGC analysis showed that the sample size of 304 cases and 1467 controls would provide the study with a power of over 98% for detecting an association of a SNP with a minor allele frequency of 0.2 or higher and per-allele odds ratio (OR) for risk allele of 1.63 or higher (estimates on rs2070803 obtained from Tokyo data set) in a 2-sided test at a significance level of .05.

In the Korea data set study, peripheral blood samples were donated from 455 patients with DGC who were diagnosed or treated at the National Cancer Center in Seoul, Korea (260 males; mean age, 52.4; 195 females; mean age, 48.5). The control subjects were 372 volunteers who participated in the National Cancer Screening Program at the National Cancer Center, Korea, and were confirmed by endoscopy not to have GC (191 males; mean age, 54.2; 181 females; mean age, 52.5). Power calculations showed that the sample size of the Korea data set would provide the study with a power of over 95% for detecting an association of rs2070803 at a significance level of .05 for the DGC study.

In the association studies (results shown in Figure 1, Table 1, and Supplementary Tables 1-4), 11 subjects (4 DGC and 2 controls from Tokyo data set, 2 controls from Aichi data set, 3 DGC cases from Korea data set) were excluded because of at least 1 missing covariate. Distributions of the covariates from subjects included in the studies are shown in Supplementary Figures 9-11.

Haplotype-based association study was performed on DNA samples from 380 DGC cases (200 males; mean age,

BASIC-ALIMENTARY TRACT